European Journal of Taxonomy 1062: 1–33
https://doi.org/10.5852/ejt.2026.1062.3286

europeanjournaloftaxonomy.eu
ISSN 2118-9773
2026 · Roy B. *et al.*

Received: 7 August 2025 • *Accepted: 19 March 2026* • *Published: 29 May 2026*

Topic editor: Tony Robillard • *Section editor: Torbjørn Ekrem* • *Desk editor: Pepe Fernández*

Research article

urn:lsid:zoobank.org:pub:631BA368-C141-48C9-B938-8A0511652787

Two new species of the genus *Eristalinus* Rondani, 1845 (Diptera: Syrphidae) from the Gangetic Plains of Eastern India

Bristi ROY[1], Oishik KAR[2], Atanu NASKAR[3,*], Jayita SENGUPTA[4] & Dhriti BANERJEE[5]

[1,2,3,4,5]Zoological Survey of India, Prani Vigyan Bhawan, M Block, New Alipore, Kolkata 700053, West Bengal, India.

[*]Corresponding author: atanudiptera@gmail.com
[1]Email: roybristi19@gmail.com
[2]Email: oishikkar10@gmail.com
[4]Email: jayitasengupta9@gmail.com
[5]Email: diptera.zsi@gmail.com

Abstract. Two new species of the hoverfly genus *Eristalinus* Rondani, 1845 (Diptera: Syrphidae) are described from West Bengal, India, based on the adult morphology of both sexes and DNA barcode data. The new species, *Eristalinus sapphirinus* Roy, Naskar & Banerjee sp. nov., is characterized by its distinctive blueish black colouration, a strongly tapering head profile towards vertex in males, and the presence of an appendix on the loop formed by R_{4+5} wing vein. The second species, *Eristalinus brunettii* Roy, Naskar & Banerjee sp. nov., was initially collected as a morphologically divergent form resembling *Eristalinus polychromata* (Brunetti, 1923), but has now been confirmed as a separate species through integrative approaches. Phylogenetic analyses using Neighbour-Joining, Maximum Likelihood, and Bayesian methods, as well as species delimitation algorithms, consistently recover *Eristalinus brunettii* as a distinct evolutionary lineage. A brief diagnosis, description, distribution, images and barcodes for both new species are provided, along with a brief diagnosis and the first description of male terminalia for *E. polychromata*, and an updated taxonomic key to the Indian *Eristalinus* is presented.

Keywords. Hoverfly, Eristalinae, taxonomy, barcoding, morphological variant, West Bengal.

Roy B., Kar O., Naskar A., Sengupta J. & Banerjee D. 2025. Two new species of the genus *Eristalinus* Rondani, 1845 (Diptera: Syrphidae) from the Gangetic Plains of Eastern India. *European Journal of Taxonomy* 1062: 1–33. https://doi.org/10.5852/ejt.2026.1062.3286

Introduction

Hoverflies (Diptera: Syrphidae), renowned for their role as pollinators, represent one of the most diverse and species-rich groups within Diptera, with over a count of 6674 described species in 284 genera worldwide (Dunn *et al.* 2020). At present, four subfamilies are recognized within Syrphidae Rondani, 1856: Microdontinae Rondani, 1845, Eristalinae Newman, 1834, Pipizinae Williston, 1885, and Syrphinae

Rondani, 1856, of which Eristalinae possess the widest range of larval habitats (Thompson & Rotheray 1998). In addition to the common feeding modes observed in syrphid larvae, such as phytophagy, coprophagy, saprophagy, and entomophagy, The Eristalinae larvae have also been reported to infest livestock and occasionally cause myiasis in vertebrates, including humans (Pérez-Bañón *et al*. 2020). Within Eristalinae, members of the genus *Eristalinus* Rondani, 1845 are notable for their distinctive eye pattern and larval association with decaying organic matter (Rotondi *et al*. 2020). The genus is distinct from other related genera by a pilose dorsomedial anepimeron, with pile equal in length to the pile on the anterior anepimeron (Ssymank *et al*. 2021). With over 75 global species, the genus is widely distributed in the Afrotropical, Australian, Palaearctic, and Oriental regions, and a few species have also been recorded from the Nearctic and Neotropical regions (Ssymank *et al*. 2021; Kondo *et al*. 2024). The genus is currently divided into five subgenera, namely, *Eristalinus* Rondani, 1845, *Eristalodes* Mik, 1897, *Helophilina* Becker, 1922, *Merodonoides* Curran, 1931, and *Oreristalis* Séguy, 1951. This genus has 14 species recorded from India, of which 11 belong to the subgenus *Eristalinus*, two in the subgenus *Eristalodes*, and only one in the subgenus *Merodonoides* (Sengupta *et al*. 2024).

Among the Indian *Eristalinus*, *Eristalinus polychromata* (Brunetti, 1923) is an endemic species originally described from West Bengal. Subsequent records have expanded its known distribution to other Indian states, including Bihar, Kerala, Himachal Pradesh, Odisha, Ladakh and Tripura (Dutta & Chakraborti 1986; Mitra *et al*. 2008, 2015; Sengupta *et al*. 2024), suggesting its adaptability across diverse ecological zones.

During several sampling campaigns conducted between 2022 and 2025 in the Gangetic Plains of Eastern India, new material of *Eristalinus* was collected. The observed morphological variation was analysed through an integrative approach. Therefore, the objective of this study is to update and refine the understanding of the *Eristalinus* diversity in India through an integrative framework, focusing on taxa allied to *E. polychromata* and Indian congeners with a unicolourous (black, blueish black or aeneous) scutellum, to better delineate species boundaries within the genus. Following this assessment, two new species of *Eristalinus* are described, the male genitalia of *E. polychromata* are documented for the first time, and the taxonomic key to the Indian species of *Eristalinus* is updated.

Material and methods

Sampling and morphological study

Specimens were collected during the day using insect sweep nets and stored in 70 % ethanol. The external morphology was first observed under a Leica EZ4 microscope following pinning and optimal stretching of the specimens for easy microscopic examination. The photographs and measurements were taken with a Leica M205A stereo iso-microscope coupled with a LEICA DFC 500 camera and Leica Application Suite LAS ver. 3.6. All measurements were taken following Choi *et al*. (2004). Male genitalia were dissected and prepared following Ricarte *et al*. (2012), and were hand-drawn under a Leica DM1000 microscope attached to a Leica k3C camera. The morphological and male genitalia terminology followed that of van Steenis *et al*. (2023). The nomenclature and subgeneric classification followed that of Systema Dipterorum (www.diptera.org), and were further aligned with the Syrphidae community website (www.syrphidae.com). Images of the holotype of *E. polychromata* were obtained from the digital archive of the NZSI available at http://zsicollections.in/. The examined materials were housed in the Diptera Section of the same collection.

Abbreviations used in the text

BOLD = Barcode of Life Data System
FH = Frons to head ratio
NZSI = Zoological Survey of India, National Zoological Collection, Kolkata, India
WM = Wing to mesonotum ratio

Molecular study

Genomic DNA (gDNA) was extracted from the right metaleg of each specimen using the QIAamp DNA Mini Kit (QIAGEN, Germany), following the manufacturer's protocol. The 5′ end of the mitochondrial Cytochrome c oxidase subunit I (COI-5′ hereafter) gene was amplified from ~20 ng of gDNA, using the universal primers LCO-1490 (forward) and HCO-2198 (reverse) (Folmer *et al*. 1994). PCR amplification conditions followed Kar *et al*. (2024). PCR was done in a total reaction volume of 50 µl comprising 20 pmol of each primer, 100 mM KCl, 20 mM Tris-HCl (pH 8.0), 1 mM DTT, 0.1 mM EDTA, 2.0 mM $MgCl_2$ 0.25 mM of each dNTP, and 1U of Taq polymerase (Takara BIO Inc., Japan). PCR-amplified products were purified using the QIAquick Gel Extraction Kit (Qiagen, Germany) following the manufacturer's instructions. Approximately 15 ng of purified PCR products was used for cycle sequencing on an ABI thermal cycler with the BigDye® Terminator ver. 3.1 Cycle Sequencing Kit (Applied Biosystems, Inc.) employing both forward and reverse primers. The cycling profile consisted of an initial denaturation at 96 °C for 1 min, followed by 25 cycles of 96 °C for 10 s, 50 °C for 5 s, and a final extension at 60 °C for 1 min 15 s. Sequencing products were purified using the BigDye X-Terminator reagent (Applied Biosystems, Inc.) and analysed on an ABI 3730 capillary genetic analyser (Banerjee *et al*. 2015; Ghosh *et al*. 2022).

Chromatograms were edited and trimmed in MEGA X (Kumar *et al*. 2018), with ambiguous regions at both ends removed. The generated sequences were matched with global sequences via GenBank and BOLD engine (Johnson *et al*. 2008) for dataset formation. In addition, all sequences were screened against the GenBank database using BLAST to confirm generic placement and to identify the closest reference sequences. A dataset comprising 35 COI-5′ sequences was constructed, incorporating six sequences generated in the present study and 29 sequences of 13 species retrieved from GenBank and BOLD (Table 1). *Eristalis tenax* (Linnaeus, 1758) was included as the outgroup. Sequence alignment was conducted using ClustalW in MEGA X, with the final aligned dataset standardized to 601 base pairs for each sequence to avoid incongruities (Kundu *et al*. 2019).

Genetic divergence and cluster analysis

The interspecific and intraspecific genetic divergences were calculated using MEGAX with the Kimura-2-Parameter (K2P) model. The best-fit nucleotide substitution model was determined using JModelTest ver. 2.1.10 (Darriba *et al*. 2012) through the CIPRES Science Gateway (Miller *et al*. 2010) and corresponding to the lowest Akaike Information Criterion (AIC) score. The best-fit nucleotide substitution model determined was the General Time Reversible model across lineages, with invariant sites and a discrete gamma distribution (GTR+I+G) (NST = 6). Phylogenetic trees were constructed using Neighbour-Joining (NJ) and Maximum Likelihood (ML) methods to represent the divergence among the tested group. MEGAX was used to construct the NJ tree, from which the bootstrap consensus tree was derived from 1000 replicates. The dataset was created and examined for ML-tree in IQ-TREE on XSEDE ver. 2.1.2 (Minh *et al*. 2020) especially for maximum-likelihood (ML) via the CIPRES website (Miller *et al*. 2012). The FigTree ver. 1.4.4 program (http://tree.bio.ed.ac.uk/software/fgtree/) was used to modify the produced tree files. As a result, the sequence divergence between the specimens was visually represented. The Bayesian Inference (BI) tree was constructed in MrBayes ver. 3.2.7a (Ronquist *et al*. 2012) with nst = 6 for the GTR+G model and metropolis-coupled Markov Chain Monte Carlo (MCMC), which was run for 1 000 000 generations with 25 % burn-in and trees saved every 100 generations, to test the reciprocal monophyletic criteria for species delimitation. Posterior probability (PP) was utilized to evaluate branch support. The iTOL ver. 6 online tool (https://itol.embl.de/) was used to construct a tree from the generated files, facilitating visual display (Letunic & Bork 2021).

Table 1. Details of sequenced individuals of species of *Eristalinus* Rondani, 1845 and *Eristalis* Latreille, 1804, with their sampling locality, coordinates, DNA vouchers, and accession and sequence numbers from GenBank and BOLD used in this study. Abbreviation: N/A = not applicable.

Species name	Locality details	Coordinates	Voucher No.	GenBank Accession No.	Sequences accessed from GenBank and BOLD
Eristalinus sapphirinus sp. nov. ♂	India, West Bengal, Hooghly	22.864° N, 87.803° E	B1	PQ622673	N/A
E. sapphirinus sp. nov. ♀	India, West Bengal, Hooghly	22.864° N, 87.803° E	B2	PQ622674	N/A
E. brunettii sp. nov. ♂	India, West Bengal, Birbhum	23.906° N, 87.527° E	B3	PQ615094	ON421642 (West Bengal, India)
E. brunettii sp. nov. ♀	India, West Bengal, Birbhum	23.906° N, 87.527° E	B4	PQ615095	
E. polychromata (Brunetti, 1923) ♂	India, West Bengal, Birbhum	23.906° N, 87.527° E	B5	PQ615097	ON226501 (West Bengal, India)
E. polychromata (Brunetti, 1923) ♀	India, West Bengal, Birbhum	23.906° N, 87.527° E	B6	PQ615099	
E. aeneus (Scopoli, 1763)	N/A	N/A	N/A	N/A	OP268184 (India), MN868834 (Portugal), MF059306 (Malta)
E. tarsalis (Macquart, 1855)	N/A	N/A	N/A	N/A	OR672772 (India), PQ327498 (India)
E. sepulchralis (Linnaeus, 1758)	N/A	N/A	N/A	N/A	MZ629004 (Finland), MZ623163 (Finland)
E. megacephalus (Rossi, 1794)	N/A	N/A	N/A	N/A	BOLD:AEJ6010 (France), MW531961 (South Africa)
E. aurulans (Wiedemann, 1824)	N/A	N/A	N/A	N/A	HM421621 (Australia), BOLD:AAI4959 (Australia)
E. tabanoides (Jaennicke, 1867)	N/A	N/A	N/A	N/A	KR830950 (Nigeria), KR830935 (Nigeria), OR674241 (India), OR674221 (India)
E. paria (Bigot, 1880)	N/A	N/A	N/A	N/A	OK444104 (India), OK655827 (India)
E. quinquestriatus (Fabricius, 1794)	N/A	N/A	N/A	N/A	ON217545 (India), MK771154 (Bangladesh)
E. fuscicornis (Karsch, 1887)	N/A	N/A	N/A	N/A	KR830994 (Nigeria), KR830993 (Nigeria)
E. quinquelineatus (Fabricius, 1781)	N/A	N/A	N/A	N/A	KR831012 (Nigeria), KR831000 (Nigeria)
E. taeniops (Wiedemann, 1818)	N/A	N/A	N/A	N/A	MN868800 (Portugal), MN868817 (Portugal)
E. arvorum (Fabricius, 1787)	N/A	N/A	N/A	N/A	OR647780 (Bangladesh), ON248238 (India)
Eristalis tenax (Linnaeus, 1758)	Outgroup				PQ328218 (India)

Species delimitation analysis

The delimitation of species was evaluated using single Poisson Tree Processes (PTP) (Zhang *et al*. 2013), Generalized Mixed Yule Coalescent (GMYC) (Pons *et al*. 2006), Automatic Barcode Gap Discovery (ABGD) (Puillandre *et al*. 2012), and Assemble Species by Automatic Partitioning (ASAP) (Puillandre *et al*. 2021). The PTP analysis was conducted on the PTP web server (https://species.h-its.org/ptp/). The ASAP technique was implemented online (https://bioinfo.mnhn.fr/abi/public/asap/). PTP employed the GTR+I+G model and Metropolis-coupled Markov Chain Monte Carlo (MCMC), which was run for 1 000 000 generations, with 100 thinning intervals and a 0.1 burn-in period, using 123 seeds. GMYC employed a single-threshold parameter for analysis. ABGD employed the Kimura (K80) ts/tv, P_{min}-P_{max} (0.001–0.1), 10 steps, and X (relative gap width) of 1.0. ASAP employed the Kimura (K80) ts/tv for assessment. The GMYC analysis was conducted on a web server version (https://species.h-its.org/gmyc/). The number of molecular operational taxonomic units (MOTUs) was ascertained using all four delimitation methodologies. A potential cohort of MOTUs was generated by each method. To confirm the congruence of the MOTUs that were generated, the subsequent two categories were implemented: (1) no match (none of the approaches identified a MOTU) and (2) match (both approaches identified a MOTU).

Results

Description of new species

Class Insecta Linnaeus, 1758
Order Diptera Linnaeus, 1758
Family Syrphidae Rondani, 1856
Subfamily Eristalinae Newman, 1834
Tribe Eristalini Newman, 1834
Genus *Eristalinus* Rondani, 1845
Subgenus *Eristalinus* Rondani, 1845

Eristalinus brunettii Roy, Naskar & Banerjee sp. nov.
urn:lsid:zoobank.org:act:4A4C7F2E-0792-4EBE-A7E1-7AD822D5A903
Figs 1–3, 7A–C

Diagnosis

The species is well distinguished from morphologically similar species by a combination of the following features: scutum entirely black, without pruinose vittae in males (Fig. 1A), or indistinct pruinose vittae sometimes present laterally in females (Fig. 3A). The anterior half of the wing has a distinct yellowish brown infuscation (Fig. 1A–B), indistinct in females (Fig. 3A). The terga are mainly orange with a black posterior margin and median vittae on terga II–III (Figs 2D, 3D). In male, the ventral margin of the surstylus is sinuous at the middle (Fig. 7C).

Etymology

The species is named after Enrico Adelelmo Brunetti to honour his immense contribution to the Indian Diptera, especially Syrphidae. The specific name *brunettii* refers to his surname and should be treated as a noun in the genitive case.

Type material

Holotype

INDIA – **West Bengal** • ♂; Hooghly, Arambagh; 22.86355° N, 87.80362° E; 15 m a.s.l.; 20 Apr. 2024; B. Roy leg.; sweep netting; GenBank no.: PQ615094; NZSI.

Paratypes

INDIA – **West Bengal** • 1 ♀; same collection data as for holotype; GenBank no.: PQ615095; NZSI • 1 ♂, 3 ♀♀; same collection data as for holotype; NZSI • 1 ♀; Murshidabad, Malipara; 24.15341° N, 88.37381° E; 40 m a.s.l.; 8 Mar. 2020; Banerjee and party leg.; pan trap; GenBank no.: ON421642; NZSI • 4 ♂♂, 3 ♀♀; Birbhum, Suri; 23.906383° N, 87.527732° E; 71 m a.s.l.; 7 Mar. 2024; B. Roy leg.; sweep netting; NZSI • 2 ♂♂, 3 ♀♀; Hooghly, Arambagh; 22.86355° N, 87.80362° E; 15 m a.s.l.; 26 May 2024; B. Roy leg.; sweep netting; NZSI.

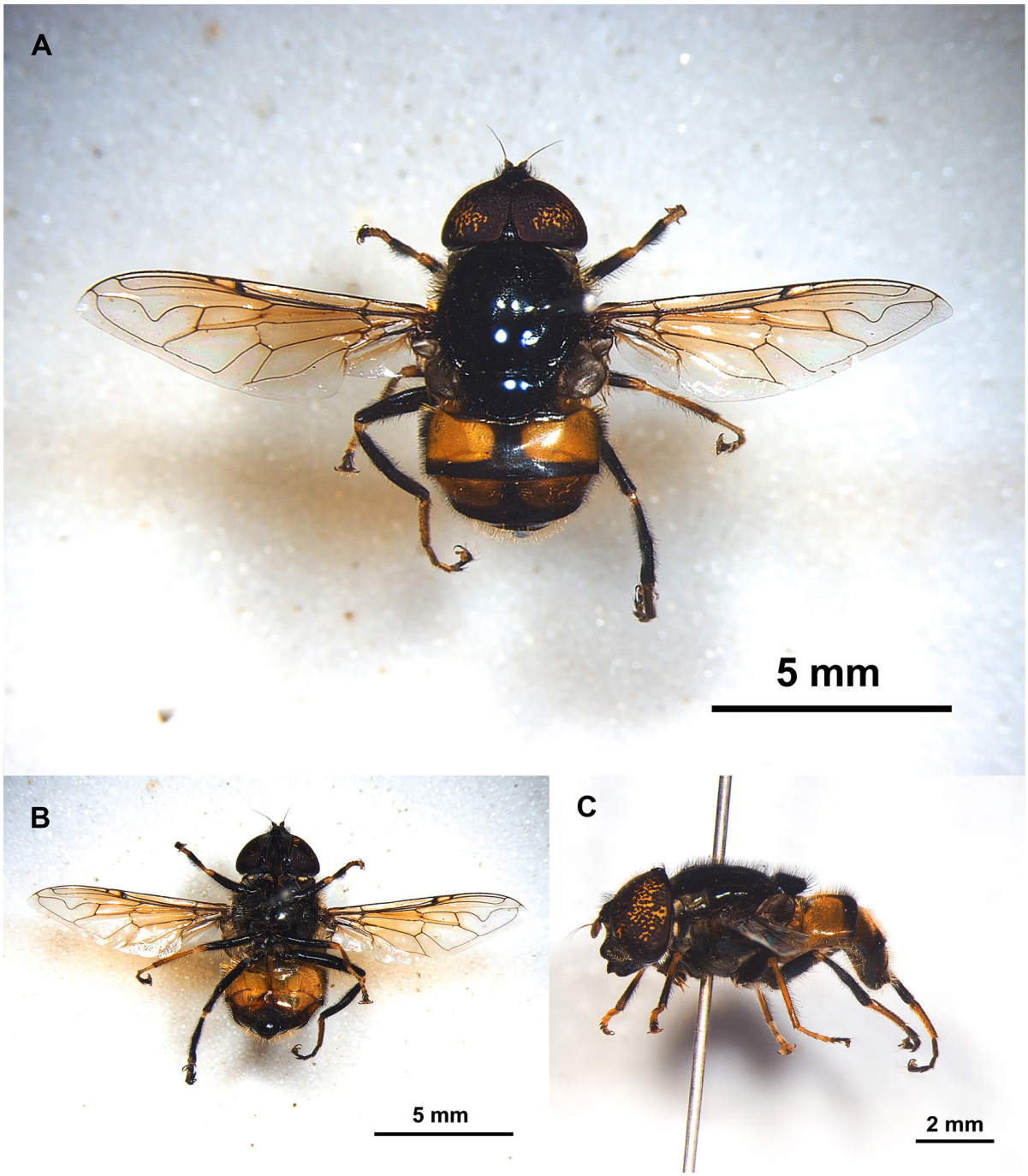

Fig. 1. *Eristalinus brunettii* Roy, Naskar & Banerjee sp. nov., holotype, ♂ (NZSI), habitus. **A**. Dorsal view. **B**. Ventral view. **C**. Lateral view.

Description

Male

Measurements. Body length 6.0–8.5 mm, wing length 5.5–7.5 mm, FH 0.19–0.24, WM 2.08–2.31.

Head (Fig. 2A–B). Eye holoptic, yellow, with dark patches, pilose on the dorsal half, eye contiguity about 12–16 facets long; vertical triangle shining black, fully occupied by ocellar triangle, entirely covered with black pile, ocelli dark red; frons shining blueish black with black pile, lateral margin narrowly pruinose; face yellowish grey pruinose with shining blueish black median vitta, facial pilosity pale yellow; facial tubercle moderately developed, gena and subcranial cavity black; occiput black with greyish white pruinosity, pilosity black dorsally and greyish white ventrally; antennae yellowish orange, postpedicel about 1.9× as long as wide, dorsal half dark brown, arista dark brown, bare.

Thorax. Mesonotum shining black with blue reflection, covered with dense, erect black pile; scutum without pruinose vittae; postpronotum and anterolateral area of scutum before transverse sulcus with pale yellow pruinosity; pleura black, with greyish white pruinosity on posterior half of anterior anepisternum, anterodorsally on posterior anepisternum, posteriorly on anepimeron, anterodorsally on katepisternum and meron; pleural pilosity pale yellow mainly, intermixed with black pile on anterodorsal part of anepimeron; anterior anepisternum and meron bare; posterior anepisternum densely pilose anterodorsally,

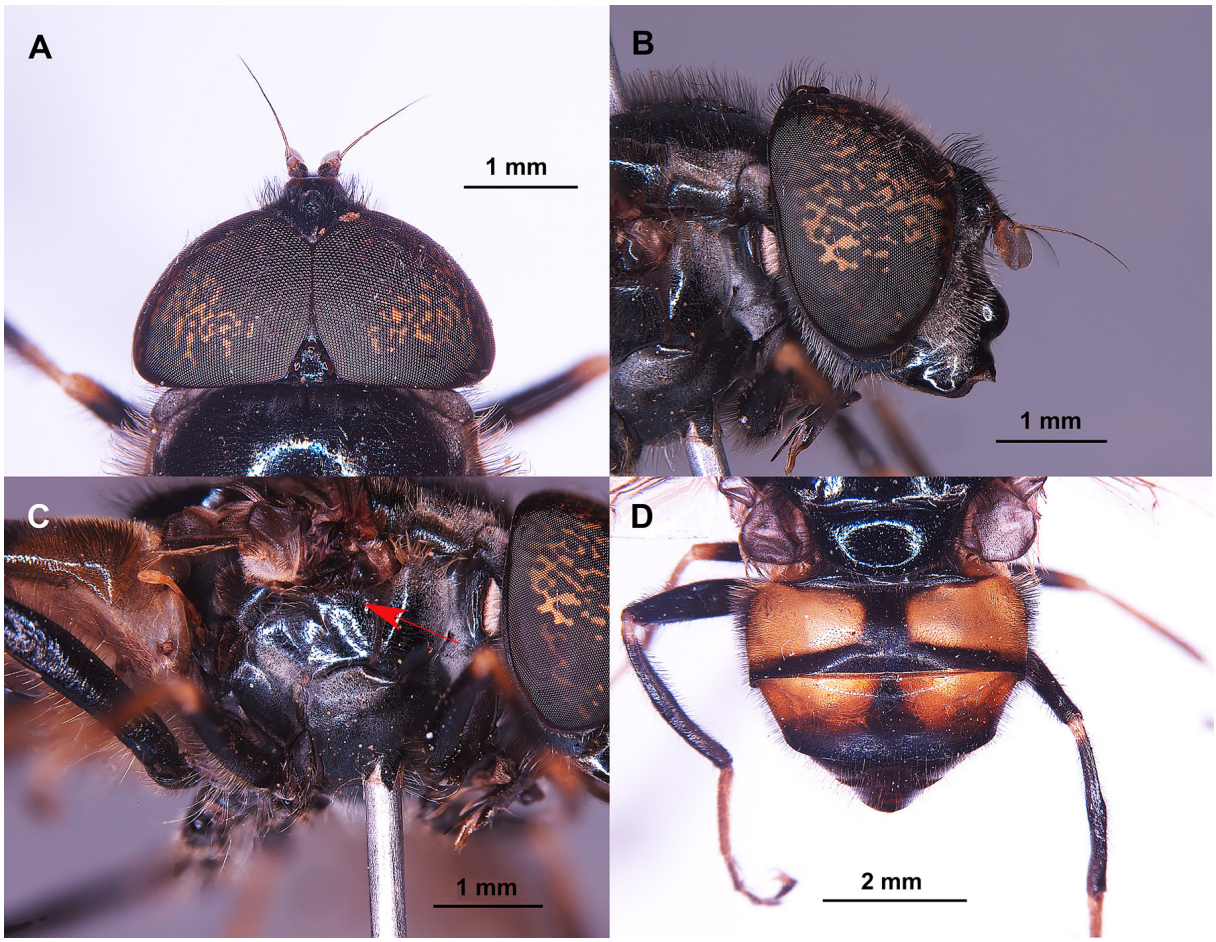

Fig. 2. *Eristalinus brunettii* Roy, Naskar & Banerjee sp. nov., holotype, ♂ (NZSI). **A**. Head, dorsal view. **B**. Head, lateral view. **C**. Thorax, lateral view (arrow showing mixed black and yellow pilosity on anepimeron). **D**. Abdomen, dorsal view.

rest of pleura comparatively sparsely pilose (Fig. 2C). Wings with distinct yellowish brown infuscation on anterior half, veins dark brown, pterostigma brown; calypters blackish grey (Fig. 1A); haltere orange. Legs mainly black; pale yellow at apex of pro- and mesofemur, apical half of protibia, whole mesotibia, extreme apex of metatibia, apical 1–2 tarsomeres of pro- and mesoleg, and basitarsomere of metaleg; pile on leg black and yellow intermixed; yellow on basal ⅔ of meso- and metafemur and basal ⅓ of profemur; black pile on rest of profemur, dorsally on pro- and mesofemur, entirely on metatibia, intermixed with yellow pile on pro- and mesotibia; pile on tarsomeres of all legs yellow and black intermixed, shorter and denser than those on femora and tibia; presence of black setulae at basolateral extreme of all tibia, and apico-laterally on all tarsomeres.

Abdomen (Fig. 2D). Abdomen yellowish orange; tergum I with shining black area at middle; terga II–III with black posterior margin and median black vittae; tergum IV with or without median black vitta and posterior margin narrower than that on terga II–III; tergum V completely black; pile on abdomen yellow, except on black part, laterally on terga II–III, and anterolateral corner of tergum II with black pile (Fig. 2D); sterna I–III yellow, rest of sterna brownish black, pilosity on sterna yellow (Fig. 1B).

Genitalia (Fig. 7A–C). Cercus sub-triangular, wider than high; surstylus rounded on extreme apex with black reclinate setulae (Fig. 7B), anteriorly with a few pile and scattered setulae, ventral margin of surstylus sinuate at the middle (Fig. 7A); hypandrium curved, almost uniformly broad throughout its

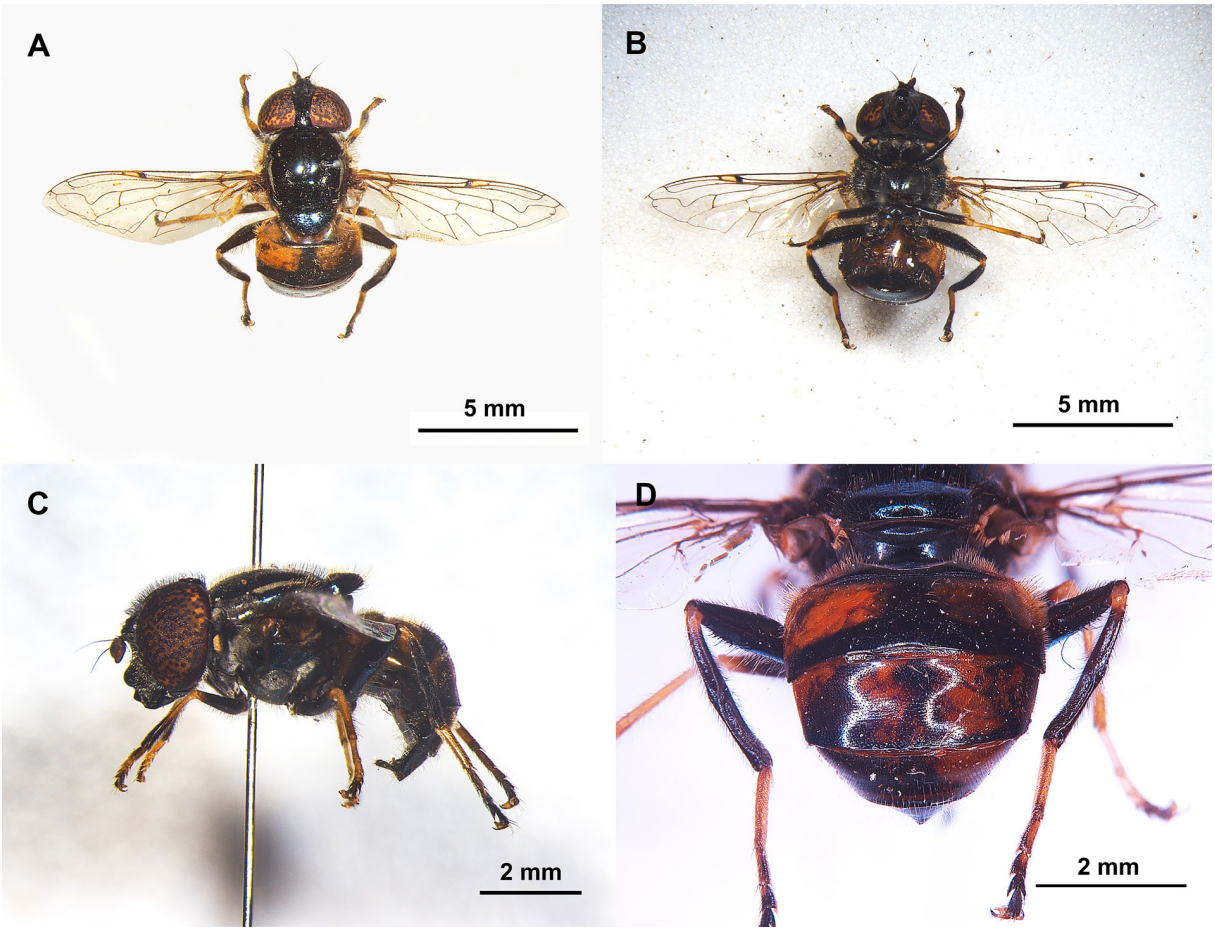

Fig. 3. *Eristalinus brunettii* Roy, Naskar & Banerjee sp. nov., paratype, ♀ (NZSI). **A**. Habitus, dorsal view. **B**. Habitus, ventral view. **C**. Habitus, lateral view. **D**. Abdomen, dorsal view.

Table 2. Differentiating features of *Eristalinus brunettii* Roy, Naskar & Banerjee sp. nov. and *Eristalinus polychromata* (Brunetti, 1923).

Characters	***E. polychromata* (Brunetti, 1923)**	***E. brunettii* sp. nov.**
Eye maculae	More or less scattered.	Clustered, appear as patches.
Facial vitta	Narrower compared to *E. brunetii* sp. nov.; occupies approximately ⅓ width of face.	Broader compared to *E. polychromata*; occupies more than ⅓ width of face.
Pruinose vittae on scutum	Present and distinct.	Absent (male) or less distinct (female).
Median black vitta on tergum III	Incomplete; only traces are present.	Complete; continuous to the posterior margin.
Body pilosity	Sparse compared to *E. brunetii* sp. nov.	Dense compared to *E. polychromata*.
Mesonotal pile in male	Yellowish brown.	Conspicuously black.
Pilosity on anepimeron	All pale yellow (Fig. 10C, marked with arrow).	Pale yellow except on the anterodorsal part, mixed with black pile (Fig. 2C, marked with arrow).
Male wing	Hyaline.	Distinct brown infuscation.
Pile on cercus	Short and sparse (Fig. 7D) compared to *E. brunetii* sp. nov.	Long and dense (Fig. 7A) compared to *E. polychromata*.
Ventral margin of surstylus	Nearly straight in the middle.	Sinuous in the middle.

length, postgonite with 2 ventral projections, one apical and one sub-medial, nearly equal in length (Fig. 7C).

Female (Fig. 3)

Body length 5.5–7.2 mm, wing length 5.8–7.0 mm, FH 0.27–0.30, WM 2.06–2.25. Similar to male except for normal sexual dimorphism and following characteristics: eye dichoptic, bare; postpedicel about 1.6× as long as wide; area anterior to vertex, frons and face along eye margins greyish white pruinose, pile on frons black; mesonotal pile yellow intermixed with black ones; tergum III with incomplete posterior margin and a trace of black vitta, pile on anterolateral corner of tergum II yellow.

Biology

Eristalinus brunettii Roy, Naskar & Banerjee sp. nov. exhibits a preference for high-flying behaviour, typically frequenting the canopies of tall woody trees such as *Mangifera indica* L. (Anacardiaceae) and *Syzygium cumini* (L.) Skeels (Myrtaceae). The species also occurs occasionally on ground-cover vegetation and agricultural lands.

Distribution

West Bengal (India).

Remarks

Specimens identified herein as *Eristalinus brunetti* sp. nov. were previously treated as morphological variants of *E. polychromata* due to similarities in the general habitus and abdominal colouration. Detailed morphological examination, however, revealed consistent differences in the body pilosity, colouration, wing infuscation, and the structure of the surstylus and postgonite, separating these specimens from *E. polychromata* (Table 2). Additionally, the female specimen ON421642 (NZSI), earlier identified as *E. polychromata* (Kar *et al*. 2024), was re-examined and found to exhibit the diagnostic characters defined for *E. brunetti*; molecular analysis further recovered this specimen within the *E. brunetti* clade. Accordingly, the specimen is here assigned to *E. brunetti* as a paratype.

Eristalinus sapphirinus Roy, Naskar & Banerjee sp. nov.
urn:lsid:zoobank.org:act:36EF7774-E588-41C7-B886-6684D385B68E
Figs 4–6, 7G–I

Diagnosis

Eristalinus sapphirinus Roy, Naskar & Banerjee sp. nov. can be distinguished from other resembling *Eristalinus* by a combination of the following features. The body is shining blueish black. In male, a sharply triangular head in the lateral view, with a smooth face profile and a weakly developed facial tubercle (Fig. 5A). Wing vein R_{4+5} with an appendix on the loop (Fig. 5D). The abdomen has yellowish brown maculae on tergum II and blueish grey on terga III–IV (Figs 5C, 6D). The male genitalia has the ventral margin curved of surstylus outward at the middle and rounded posteriorly (Fig. 7I).

Etymology

The specific name is from Latin *sapphirinus* ('sapphire-coloured') and indicates the shining blueish black sheen of the species.

Type material

Holotype

INDIA – **West Bengal** • ♂; Hooghly, Arambagh; 22.86474° N, 87.80363° E; 15 m a.s.l.; 22 Nov. 2022; B. Roy leg.; sweep netting; GenBank no.: PQ622673; NZSI.

Paratypes

INDIA – **West Bengal** • 1 ♀; Hooghly, Arambagh; 22.86355° N, 87.80362° E; 15 m a.s.l.; 20 Apr. 2024; B. Roy leg.; sweep netting; GenBank no.: PQ622674; NZSI • 1 ♂, 5 ♀♀; Hooghly, Arambagh; 22.86355° N, 87.80362° E; 15 m a.s.l.; 20 Apr. 2024; B. Roy leg.; sweep netting; NZSI • 4 ♂♂, 5 ♀♀; Hooghly, Arambagh; 22.86355° N, 87.80362° E; 15 m a.s.l.; 28 Mar. 2025; B. Roy leg.; sweep netting; NZSI • 1 ♀; Hooghly, Arambagh; 22.86309° N, 87.80278° E; 15 m a.s.l.; 13 Jun. 2025; B. Roy leg.; sweep netting; NZSI.

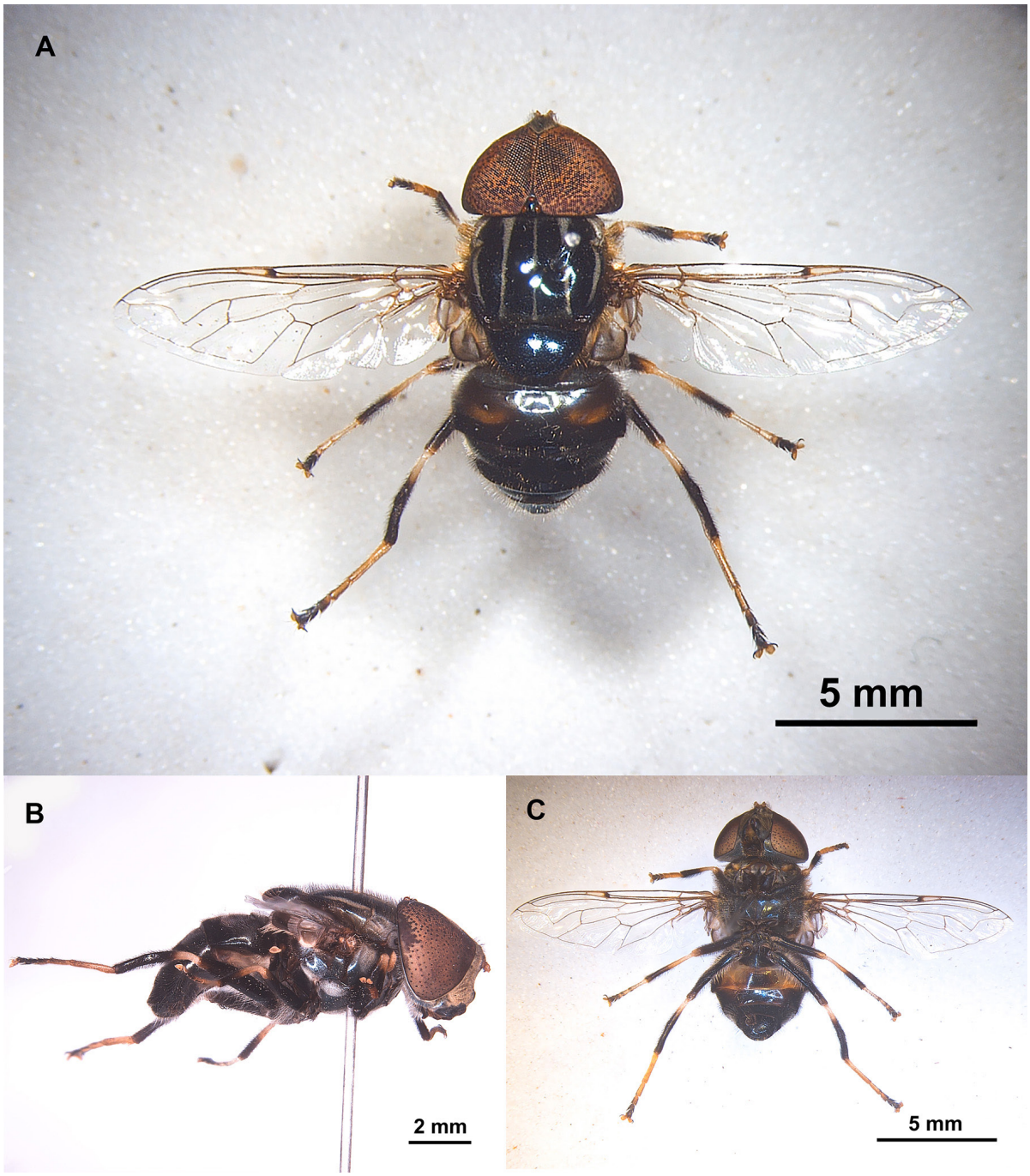

Fig. 4. *Eristalinus sapphirinus* Roy, Naskar & Banerjee sp. nov., holotype, ♂ (NZSI), habitus. **A**. Dorsal view. **B**. Ventral view. **C**. Lateral view.

Description

Male

Measurements. Body length 9.9–10.2 mm, wing length 8.5–8.8 mm, FH 0.21–0.23, WM 2.10–2.20.

Head. Head sharply triangular laterally, strongly tapering towards vertex (Fig. 5A); eye greenish yellow with tiny purple maculae, pilose on dorsal half, eye contiguity about 19–22 facets long, eye facets larger on dorsal part; vertical triangle shining black with dark brown pile, ocelli reddish orange; frons and face with yellowish grey pruinosity, pilosity on frons black and pale yellow on face, facial tubercle poorly developed, black and bare; gena yellowish grey pruinose, subcranial cavity brown; occiput with greyish white pruinosity, with black pile dorsally and greyish white pile ventrally; antennae orange, postpedicel about 1.9× as long as wide, orange-yellow with dark brown dorsal margin, arista bare, brownish orange, darker apically (Fig. 5A).

Thorax. Mesonotum shining blueish black, covered with yellowish brown pile, intermixed with black pile on notopleuron, lateral side of scutum after transverse sulcus, and lateral margin of scutellum, pile longer on pleura, sterna and posterior margin of scutellum; scutum with 5 longitudinal yellowish grey pruinose vittae (Fig. 4A); pleura with greyish white pruinosity on postpronotum, notopleuron, posteriorly

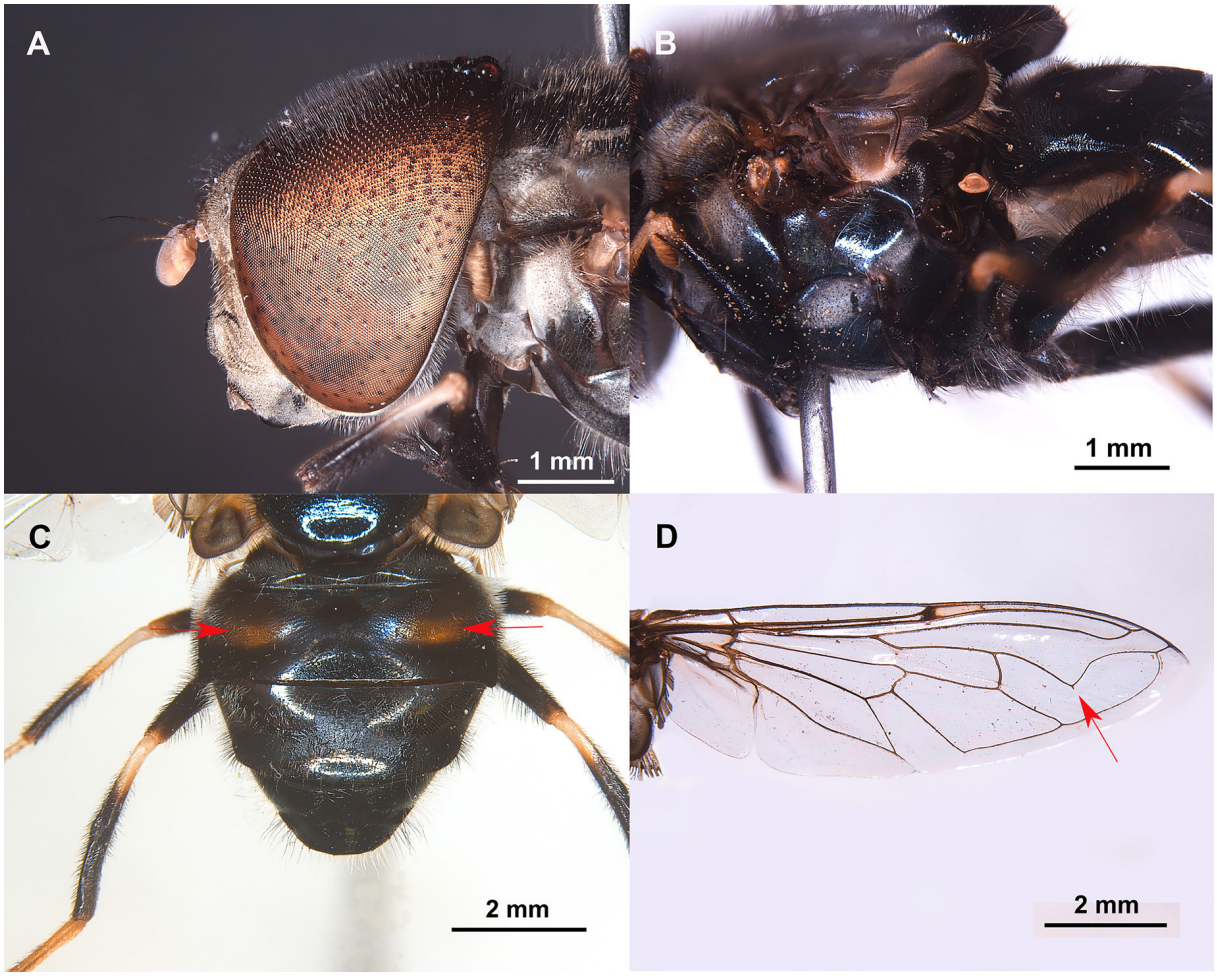

Fig. 5. *Eristalinus sapphirinus* Roy, Naskar & Banerjee sp. nov., holotype, ♂ (NZSI). **A**. Head, lateral view. **B**. Thorax, lateral view. **C**. Abdomen, dorsal view (arrows indicate yellowish brown maculae on tergum 2). **D**. Wing (arrow indicate the appendix on the loop of vein R_{4+5}).

on anterior anepisternum, upper part of anepimeron and posterior anepisternum (Fig. 5B); pleural pilosity pale yellow; anterior anepisternum and meron bare; posterior anepisternum densely pilose anterodorsally, remaining pleura comparatively sparsely pilose (Fig. 5B). Wings hyaline, stigma pale, vein R_{4+5} curved, with appendix at its extreme lower point (Fig. 5D); upper and lower calypter blackish grey, with dark margins (Fig. 4A); haltere pale yellow. Legs mainly black; pale yellow at the apex of all femora, basal ½ of pro- and mesotibia, basal ⅓ of metatibia and 1–3 tarsomeres of all legs (Fig. 4C); presence of black pile anteriorly on procoxa and trochanter, anteroventrally on mesocoxa and anteriorly on mesotrochanter; femora and tibiae with denser and longer black pile on black part and comparatively shorter and sparser pale yellow pile on pale yellow part; ventral surface of meso- and metafemur with longer pale yellow pile compared to rest of leg pilosity; black setulae present apically on all tibiae, apicolaterally on protarsomeres, ventrally and apicolaterally on mesotarsomeres, laterally on metatarsomeres.

Abdomen. Ovate, shining blueish black, finely punctate on dorsal surface; tergum I shining black, grey pruinose; tergum II with transverse, yellowish brown maculae (Fig. 5C) and dull black, arcuate fascia, reaching posterior margin laterally, leaving blueish grey posterior margin in middle; terga III–IV similar to tergum II, except shining blueish grey maculae; tergum V shining blueish grey; abdominal pilosity mainly yellowish white, more distinct laterally, black pile present posterolaterally on tergum II; sternum II pale yellow, with remaining sterna shining black, pilosity on sterna yellowish white.

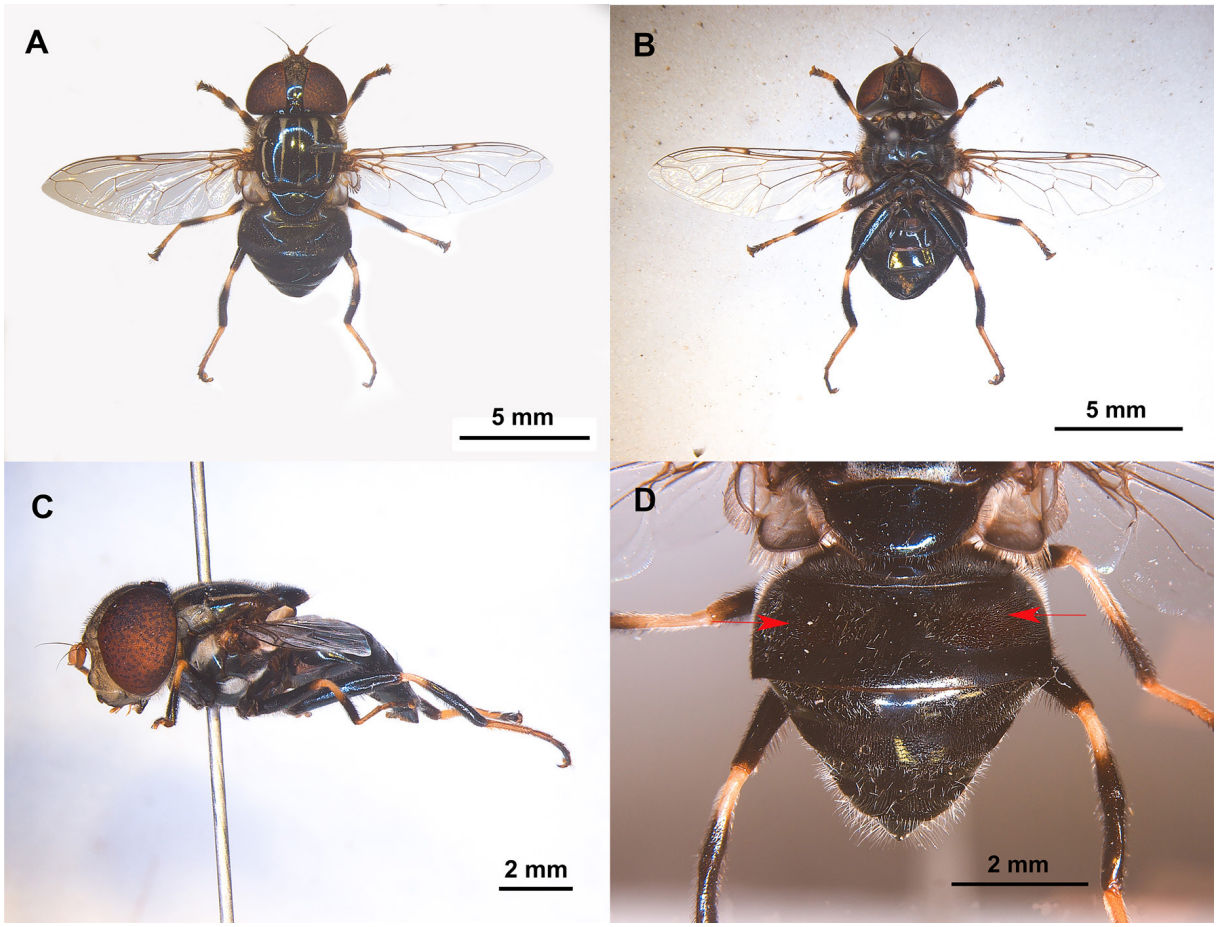

Fig. 6. *Eristalinus sapphirinus* Roy, Naskar & Banerjee sp. nov., paratype, ♀ (NZSI). **A**. Dorsal habitus. **B**. Ventral habitus. **C**. Lateral habitus. **D**. Abdomen, dorsal view (arrows indicate dark brown maculae on tergum 2).

Genitalia (Fig. 7G–I). Cercus nearly square-like (Fig. 7G), wider than high; apex of surstylus rounded with black reclinate setulae, anteriorly with a few pile and scattered setulae (Fig. 7G–H), ventral margin expanded and curved outward at middle and rounded posteriorly; hypandrium curved, suddenly narrowing towards apex, postgonite with 2 ventral projections, one large hook-shaped projection apically and one small incurved hook, submedially (Fig. 7I).

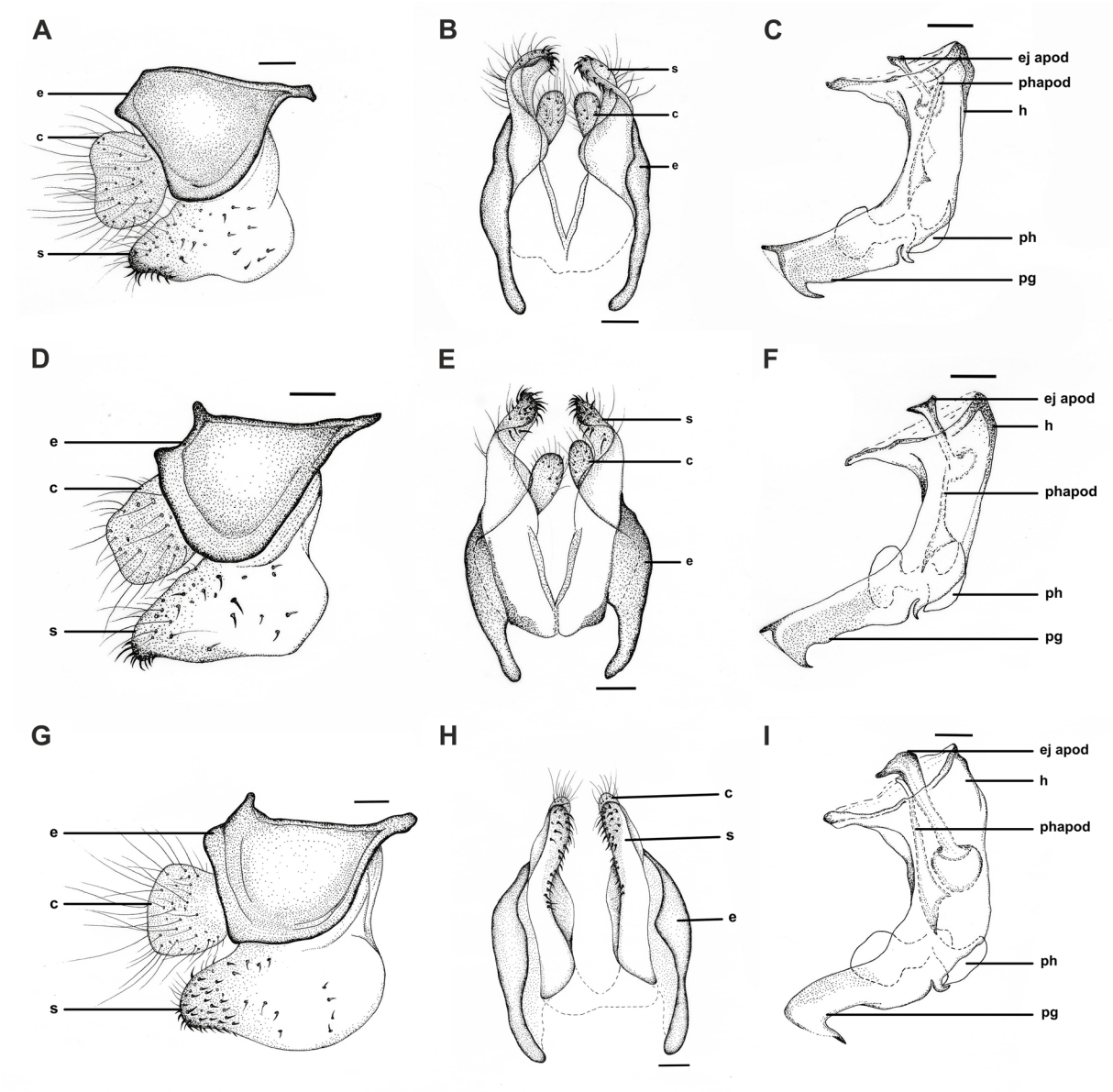

Fig. 7. Male genitalia of *Eristalinus*. **A–C**. *E. brunettii* Roy, Naskar & Banerjee sp. nov., paratype, ♂ (NZSI). **A**. Epandrium, lateral view. **B**. Epandrium, ventral view. **C**. Hypandrium, lateral view. **D–F**. *E. polychromata* (Brunetti, 1923), ♂ (NZSI). **D**. Epandrium, lateral view. **E**. Epandrium, ventral view. **F**. Hypandrium, lateral view. **G–I**. *E. sapphirinus* Roy, Naskar & Banerjee sp. nov., paratype, ♂ (NZSI). **G**. Epandrium, lateral view. **H**. Epandrium, ventral view. **I**. Hypandrium, lateral view. Abbreviations: c = cercus; e = epandrium; ej apod = ejaculatory apodeme; h = hypandrium; pg = postgonite; ph = phallus; phapod = phallapodeme; s = surstylus. Scale bars = 0.1 mm.

Female (Fig. 6)

Body length 8.9–9.7 mm, wing length 7.8–8.3 mm, FH 0.26–0.30, WM 2.05–2.23. Similar to males except for normal sexual dimorphism and following characteristics: eyes dichoptic, bare; postpedicel about 1.7 × as long as wide; maculae on tergum II dark brown (Fig. 6D); all sterna shining blueish black (Fig. 6B).

Biology

The species was first recorded in November 2022, feeding on *Mikania micrantha* Kunth (Asteraceae) blooms along a roadside drainage channel in a locality of West Bengal. Subsequent observations in April 2024 and March 2025 in the same locality documented small aggregations, primarily of females, co-occurring with congeners —*Eristalinus arvorum* (Fabricius, 1787), *E. megacephalus* (Rossi, 1794), and *E. brunettii* sp. nov.— on a medium-sized *Streblus asper* Lour. (Moraceae) tree adjacent to a domestic drainage system and close to sesame (Pedaliaceae) cultivation. Females were frequently observed exhibiting slow hovering flight and prolonged floral visitation, making them more readily collectible than the agile males. Additionally, a solitary female was collected in June 2025 from a nearby sesame crop field.

Distribution

West Bengal (India).

Remarks

Eristalinus sapphirinus sp. nov. shows morphological affinities with several Indian congeners bearing a unicolourous (black, blueish black or aeneous) scutellum, but can be readily distinguished by its shining blueish black body with yellowish brown to dark brown maculae restricted to abdominal tergum II and the presence of an appendix on the loop of vein R_{4+5}. It differs from *Eristalinus tarsalis* (Macquart, 1855), which has conspicuous creamy white maculae or fasciae on the abdominal terga, by the complete absence of such markings and by its metallic blueish colouration. Among the aeneous-bodied species such as *E. aeneus* (Scopoli, 1763) and *E. sepulchralis* (Linnaeus, 1758), it is similar to them in lacking creamy abdominal markings, but differs by its vivid blueish sheen and the presence of yellowish brown to dark brown maculae on tergum II. The new species also exhibits a close affinity in the male genital morphology to *E. polychromata* and its allied species *E. brunettii* sp. nov., in the arched hypandrium and elongate, apicoventrally hooked postgonite with a distinct subventral projection; however, in *E. sapphirinus*, the ventral margin of the surstylus is curved outward medially and rounded posteriorly, while it is distinctly sinuous medially in *E. brunettii* and nearly straight in *E. polychromata*. Externally, *E. sapphirinus* can be further distinguished from *E. polychromata* and *E. brunettii* by its predominantly blueish black body with yellowish brown maculae confined to tergum II. In contrast, both *E. polychromata* and *E. brunettii* possess orange abdominal terga with black posterior margins and distinct or indistinct median vittae.

Apart from this, the male genitalia of *Eristalinus sapphirinus* sp. nov. share similarities with those of *E. megacephalus*, particularly in the structure of the epandrium, surstylus, and the curvature of the hypandrium, but differ in the configuration of the postgonite, and exhibit a marked similarity with *E. taeniops* (Wiedemann, 1818) in the structure of the hypandrium and postgonite (Pérez-Bañón *et al.* 2003).

Remarks on other Eristalinus from India

Eristalinus polychromata (Brunetti, 1923)
Figs 8–11, 7D–F

Eristalis polychromatus Brunetti, 1923: 180.

Diagnosis

Small to medium-sized species (5.0–7.2 mm). Male: eyes holoptic, pilose on dorsal half; postpedicel brownish orange, longer than wide with dark brown dorsal margin (Fig. 10A–B); mesonotum shining

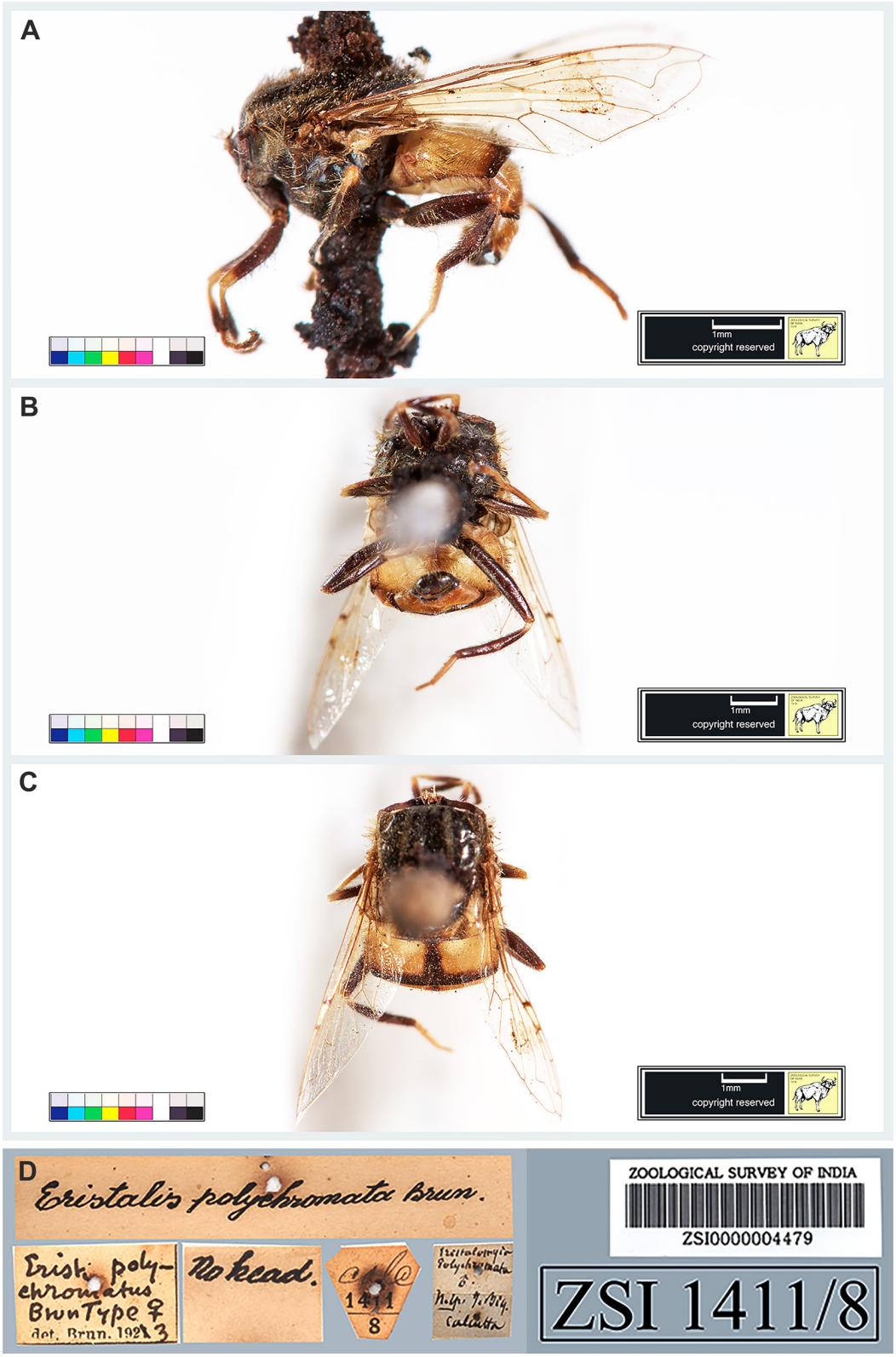

Fig. 8. *Eristalinus polychromata* (Brunetti, 1923), holotype, ♂ (NZSI), habitus (head missing), obtained from the digital archive of the NZSI; https://zsicollections.in/specimen/ZSI0000004479. **A**. Lateral view. **B**. Ventral view. **C**. Dorsal view. **D**. Holotype label. Scale bar = 1 mm. The image is reproduced with permission from NZSI and in accordance with *EJT*'s guidelines.

black, scutum with four distinct pruinose vittae (Fig. 9A); mesonotal pile yellow, intermixed with black ones (Fig. 9C); pleural pilosity all yellow (Fig. 10C); wing nearly hyaline (Fig. 9A), without distinct infuscation, though brownish tinge sometimes may present; abdomen mainly orange, tergum II with black posterior margin and distinct median black vitta, terga III–IV with narrow posterior margin (compared to tergum II), without median vittae, sometimes traces of median vitta may present anteriorly on tergum III, tergum V black (Fig. 10D); male genitalia (Fig. 7D–F): mid-ventral margin of surstylus nearly straight (Fig. 7D), hypandrium narrowing towards apex, postgonite with 2 ventral projections (Fig. 7F). Female: eyes dichoptic, bare; tergum III with distinct, black posterior margin and median vitta (Fig. 11).

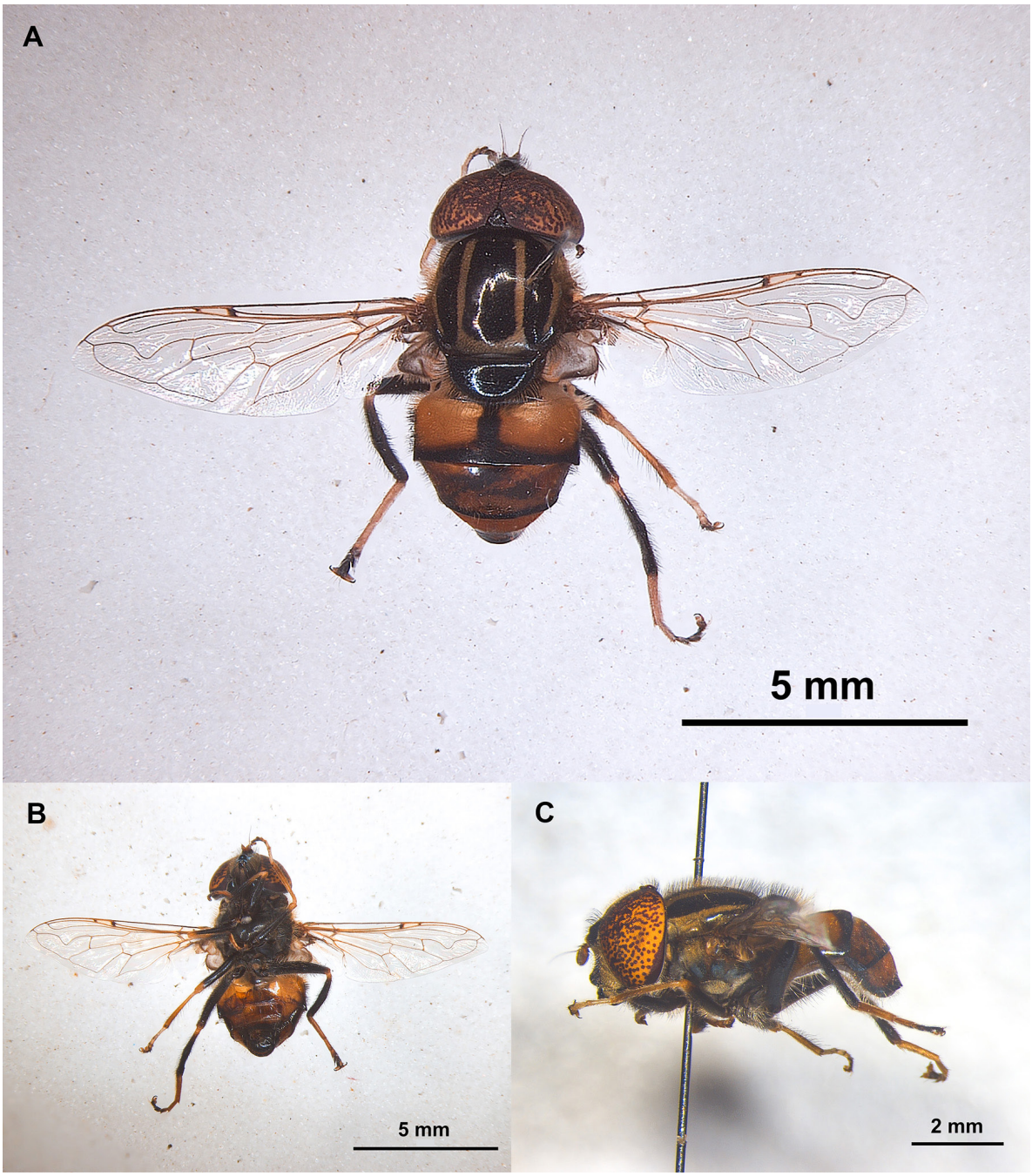

Fig. 9. *Eristalinus polychromata* (Brunetti, 1923), ♂ (NZSI), habitus. **A**. Dorsal view. **B**. Ventral view. **C**. Lateral view.

Type material

Holotype (Fig. 8)
INDIA • 1 ♂; Calcutta; J. Bigot; NZSI, ZSI1411/8.

Other material examined

INDIA – **West Bengal** • 2 ♂♂, 6 ♀♀; Hooghly, Arambagh; 22.86355° N, 87.80362° E; 15 m a.s.l.; 26 Jun. 2022; B. Roy leg; sweep netting; NZSI • 7 ♂♂, 4 ♀♀; Birbhum, Suri; 23.906383° N, 87.527732° E; 71 m a.s.l.; 7 Mar. 2024; B. Roy leg.; sweep netting; NZSI.

Description of male genitalia

Cercus squarish; surstylus rounded on extreme apex, with black reclinate setulae (Fig. 7H), ventral margin of surstylus nearly straight at middle (Fig. 7G); hypandrium curved, narrowing apically, postgonite with two ventral projections, apical one forms a crescent-shaped curve rather than hook, submedial projection hook-shaped (Fig. 7I).

Biology

The species exhibits predominantly ground-level activity and a strong association with low vegetation and crop fields. Individuals were frequently seen visiting plants, e.g., *Phyla nodiflora* (L.) Greene (Ver-

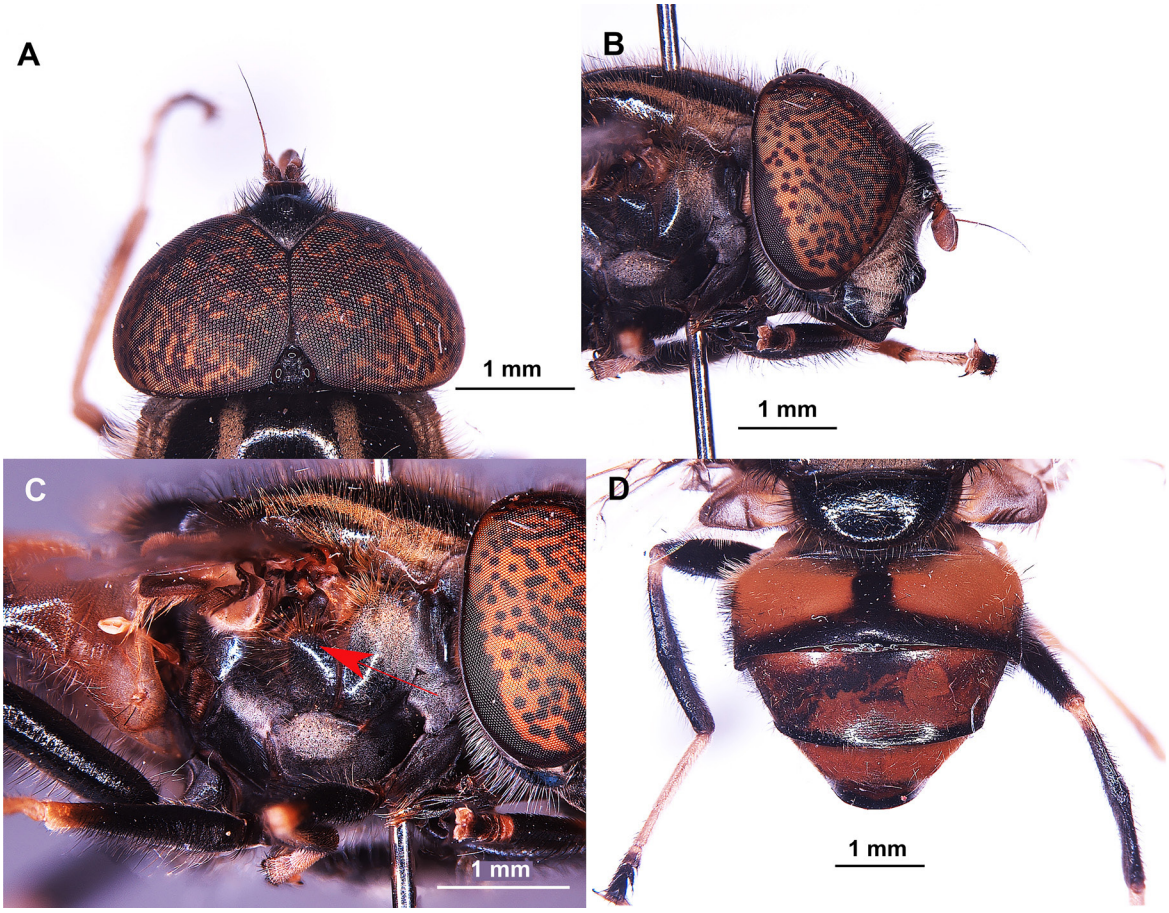

Fig. 10. *Eristalinus polychromata* (Brunetti, 1923), ♂ (NZSI). **A**. Head, dorsal view. **B**. Head, lateral view. **C**. Thorax, lateral view (arrow showing yellow pilosity on anepimeron). **D**. Abdomen, dorsal view.

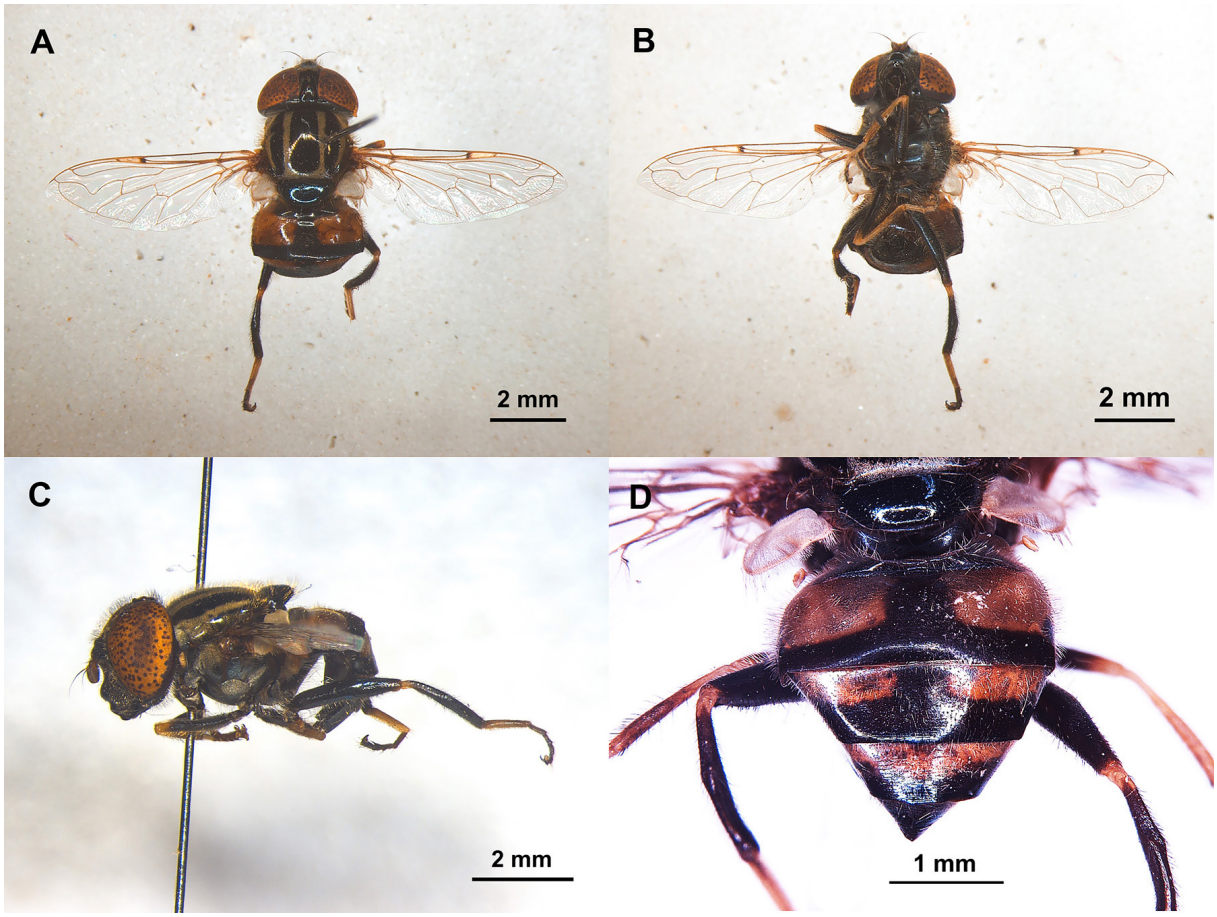

Fig. 11. *Eristalinus polychromata* (Brunetti, 1923), ♀ (NZSI). **A**. Dorsal habitus. **B**. Ventral habitus. **C**. Lateral habitus. **D**. Abdomen.

benaceae), *Mimosa pudica* L. (Fabaceae) and *Croton bonplandianus* Baill. (Euphorbiaceae). Occasional co-occurrence on ground-cover vegetation with *E. brunettii* sp. nov. was also observed.

Distribution

Bihar, Himachal Pradesh, Kerala, Odisha, Tripura, West Bengal (India).

Remarks

Both males and females of *E. polychromata* share similarities with *E. brunettii* sp. nov. in the general appearance of the body; mainly orange abdominal terga with black posterior margins and median vittae, the complete absence of creamy white markings on abdomen, and the shape of the hypandrium and projections of postgonite. However, the two species can be readily distinguished by the characters summarized in Table 2.

Key to Indian species of the genus Eristalinus (males and females)

Eristalinus quadristriatus (Macquart, 1846) is excluded from this key because no reliably identified specimens have been available for examination, and its original description is too brief to allow a confident assessment of its diagnostic characters.

1. Metafemora distinctly incrassate and arcuate, yellow with a median brown ring; metatibiae firmly compressed and carinate on basoventral ⅓ (Fig. 12A–B) (subgenus ***Merodonoides***) .... ***Eristalinus fasciatus*** (Macquart, 1834)
– Metafemora at most slightly incrassate, not arcuate; metatibiae neither compressed nor carinate on basoventral ⅓ (other subgenera) (Fig. 12C–D) 2

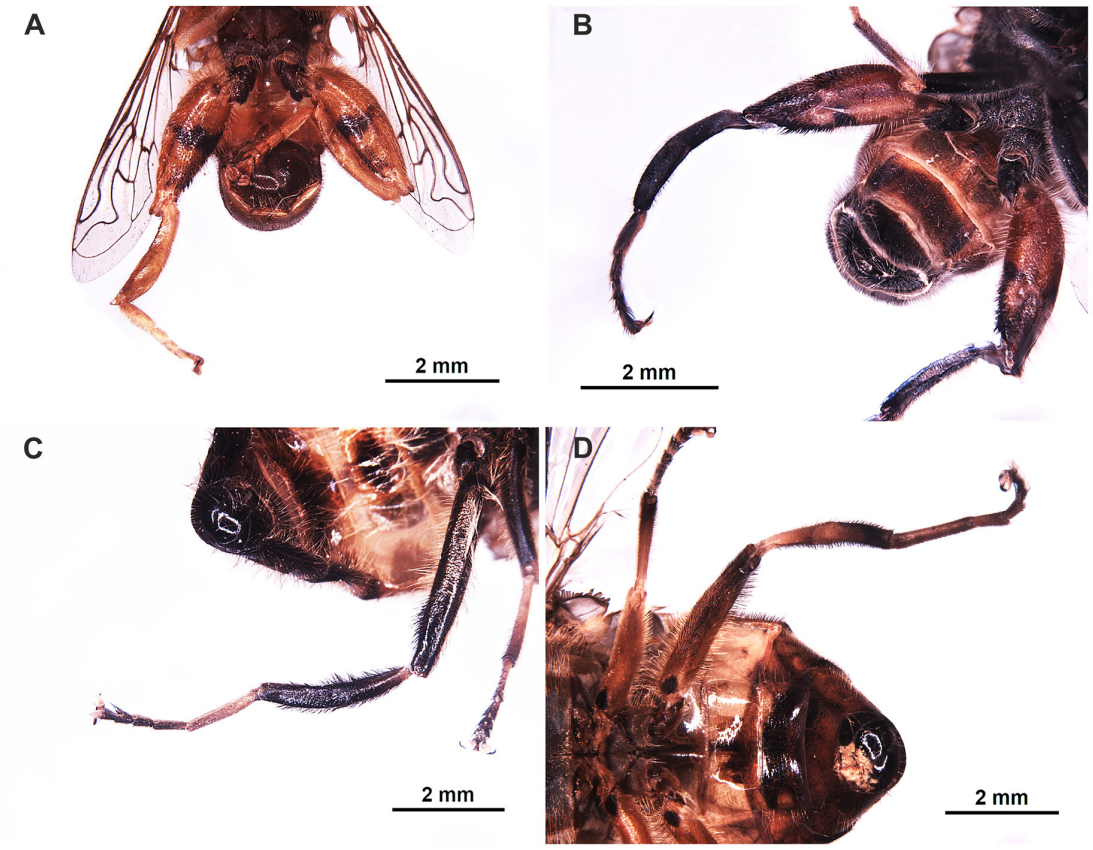

Fig. 12. Ventral view of metaleg. **A–B**. *Eristalinus fasciatus* (Macquart, 1834) (NZSI). **A**. Male. **B**. Female. **C**. *E. paria* (Bigot, 1880), ♂. **D**. *E. arvorum* (Fabricius, 1787), ♂.

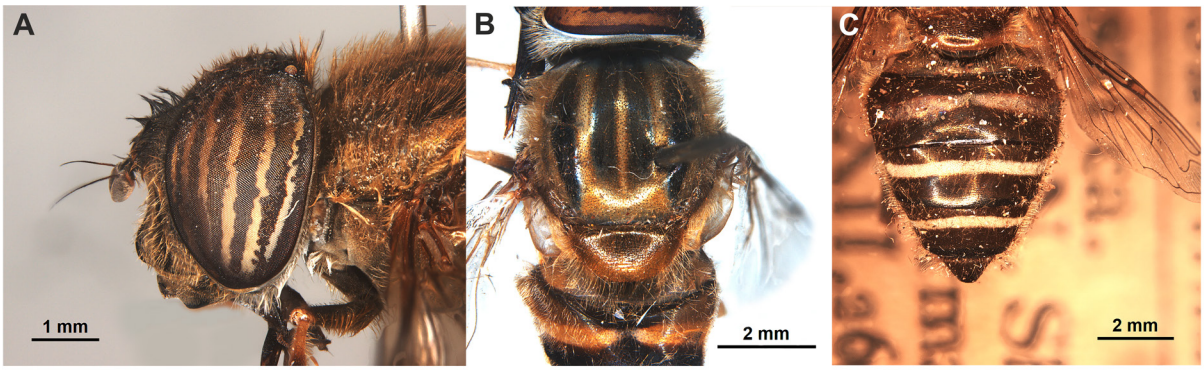

Fig. 13. *Eristalinus paria* (Bigot, 1880), ♂ (NZSI). **A**. Head, lateral view. **B**. Thorax, dorsal view. **C**. Female abdomen, dorsal view.

2. Eyes fasciate and maculate (subgenus ***Eristalodes***) (Fig. 13A) 3
– Eyes maculate (subgenus ***Eristalinus***) (Figs 2B, 5A) 4

3. Scutum dull yellowish grey with four indistinct black vittae; tergum II with a broad uninterrupted yellow fascia bordered narrowly with black anterior and posterior margins (Kondo *et al*. 2024: fig. 2a) .....***Eristalinus taeniops*** (Wiedemann, 1818)
– Scutum pale yellow with four distinct black vittae (Fig. 13B); tergum II mostly black, with a narrow creamy white fascia interrupted medially (Fig. 13C) .....***Eristalinus paria*** (Bigot, 1880)

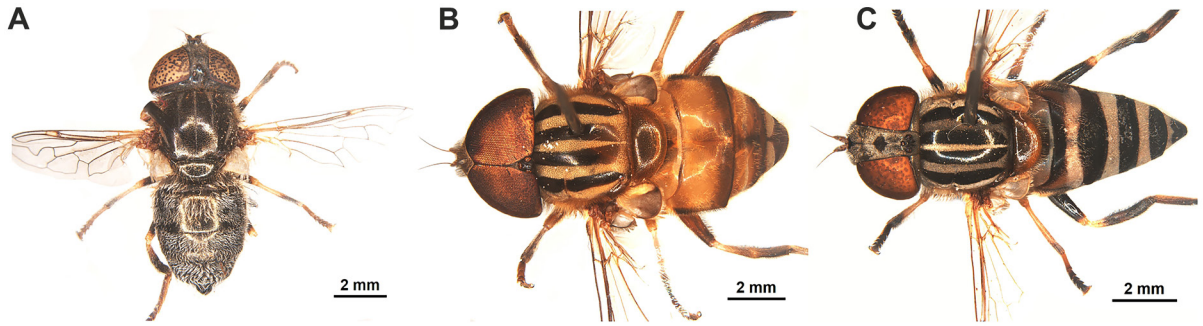

Fig. 14. Dorsal habitus. **A**. *Eristalinus aeneus* (Scopoli, 1763), ♀ (NZSI). **B**. *E. arvorum* (Fabricius, 1787), ♂ (NZSI). **C**. *E. tabanoides* (Jaennicke, 1867), ♀ (NZSI).

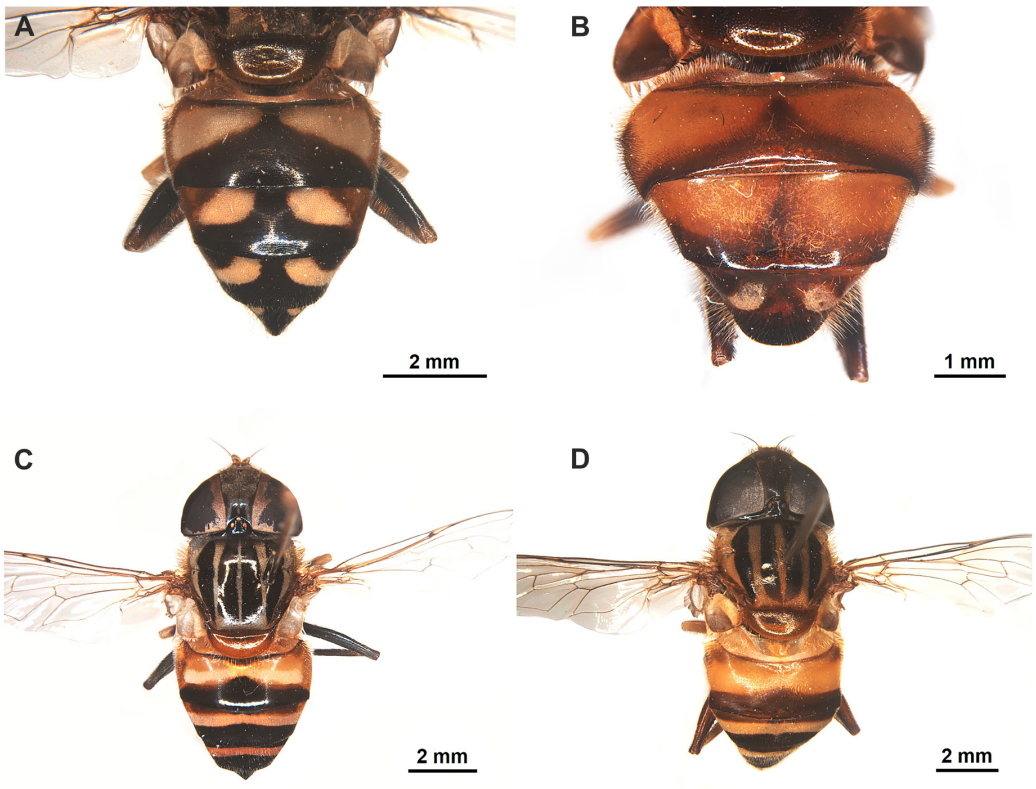

Fig. 15. Abdomen, dorsal view. **A–B**. *Eristalinus obliquus* (Wiedemann, 1824) (NZSI). **A**. Female. **B**. Male. **C–D**. Dorsal habitus. **C**. *E. quinquestriatus* (Fabricius, 1794), ♀ (NZSI). **D**. *E. arvorum* (Fabricius, 1787), ♂ (NZSI).

4. Abdomen metallic green, without markings (Fig. 14A) 5
– Abdomen with coloured markings, at least on tergum II (Figs 5C, 6D, 14B–C) 6

5. Abdomen uniformly aeneous green, entirely covered with pale yellow pile and without markings (Fig. 14A); male holoptic .....***Eristalinus aeneus*** (Scopoli, 1763)
– Abdomen mostly dull black, with pale yellow pile only on lateral and posterior margin of each tergum; terga II–III with aeneous maculae (Kahanpää, 2021: figs 1a, 3); male dichoptic ....***Eristalinus sepulchralis*** (Linnaeus, 1758)

6. Scutellum unicoloured (Figs 1A, 3A, 4A, 6A, 9A, 11A) 7
– Scutellum, at least partly from yellow to translucent (Fig. 15) 10

7. Terga mainly black, always with creamy white maculae (Ka-Lun, 2022: figs 11–12) ....***Eristalinus tarsalis*** (Macquart, 1855)
– Terga differently coloured, without creamy white markings (at most tergum II with orange/yellowish brown maculae) (Figs 2D, 3D, 5C, 6D, 10D, 11D) 8

8. Terga II–IV with conspicuous orange maculae, a black fascia posteriorly, and sometimes with median black vittae (Figs 2D, 3D, 10D, 11D) 9
– Only tergum II with yellowish brown maculae (more distinct in males), rest of the terga with shiny blueish grey maculae and arcuate black fascia posteriorly (Figs 5C, 6D) ....***Eristalinus sapphirinus*** Roy, Naskar & Banerjee sp. nov.

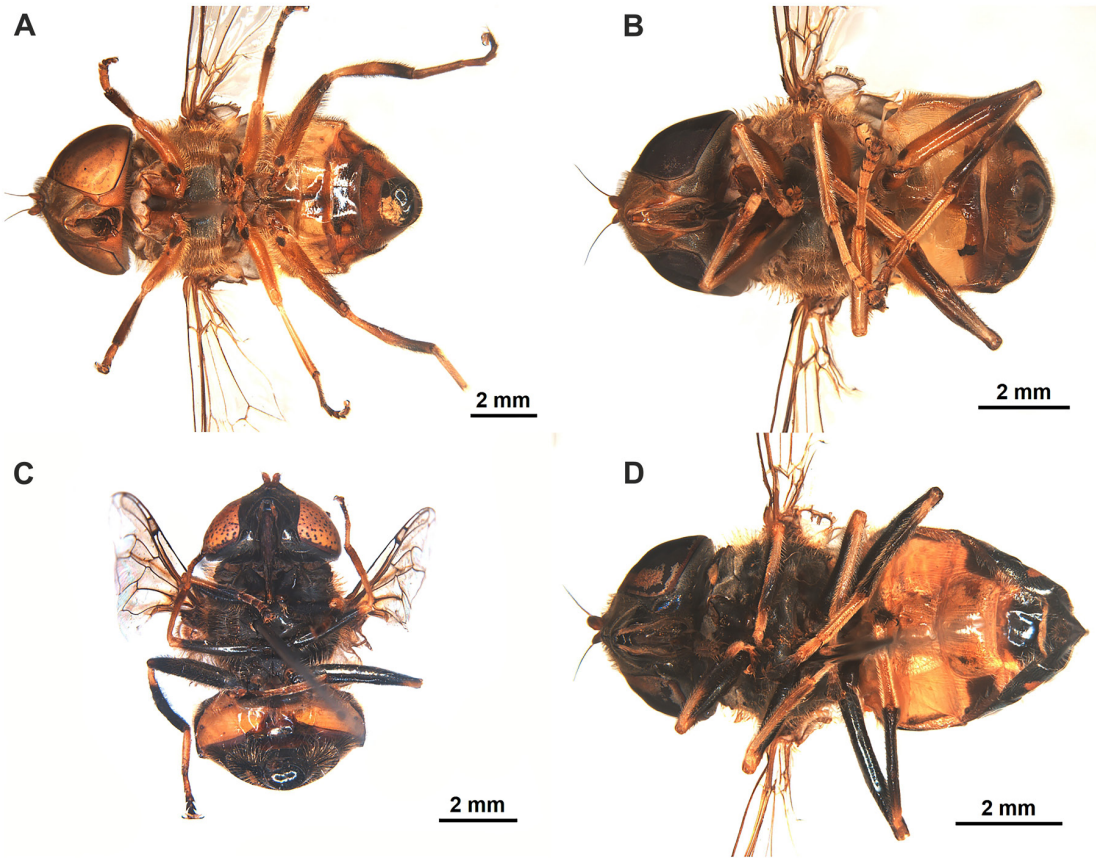

Fig. 16. Ventral habitus. *Eristalinus arvorum* (Fabricius, 1787), (NZSI). **A**. Male. **B**. Female. **C–D**. *E. quinquestriatus* (Fabricius, 1794) (NZSI). **C**. Male. **D**. Female.

9. Males: scutum uniformly shining black without pruinose vittae, mesonotal pile long, dense and black; tergum III with distinct median black vitta; wing with a distinct brown infuscation (Fig. 1A–C). Females: indistinct pruinose vittae may present laterally on scutum (Fig. 3A) ....***Eristalinus brunettii*** Roy, Naskar & Banerjee sp. nov.
– Scutum with four distinct, pruinose vittae in both sexes (Figs 9A, 11A); Males: mesonotal pile short, sparse, and yellowish brown; tergum III with median black vitta indistinct or absent; wings nearly hyaline (Fig. 9A–C) .....***Erisalinus polychromata*** (Brunetti, 1923)

10. Terga with obliquely placed creamy white markings (Fig. 15A–B) ....***Eristalinus obliquus*** (Wiedemann, 1824)
– Terga with transversely placed creamy white markings (Fig. 15C–D) 11

Fig. 17. Abdomen, dorsal view. **A–B**. *Eristalinus quinquestriatus* (Fabricius, 1794) (NZSI). **A**. Male. **B**. Female. **C**. Dorsal habitus of *E. megacephalus* (Rossi, 1794), ♂ (NZSI).

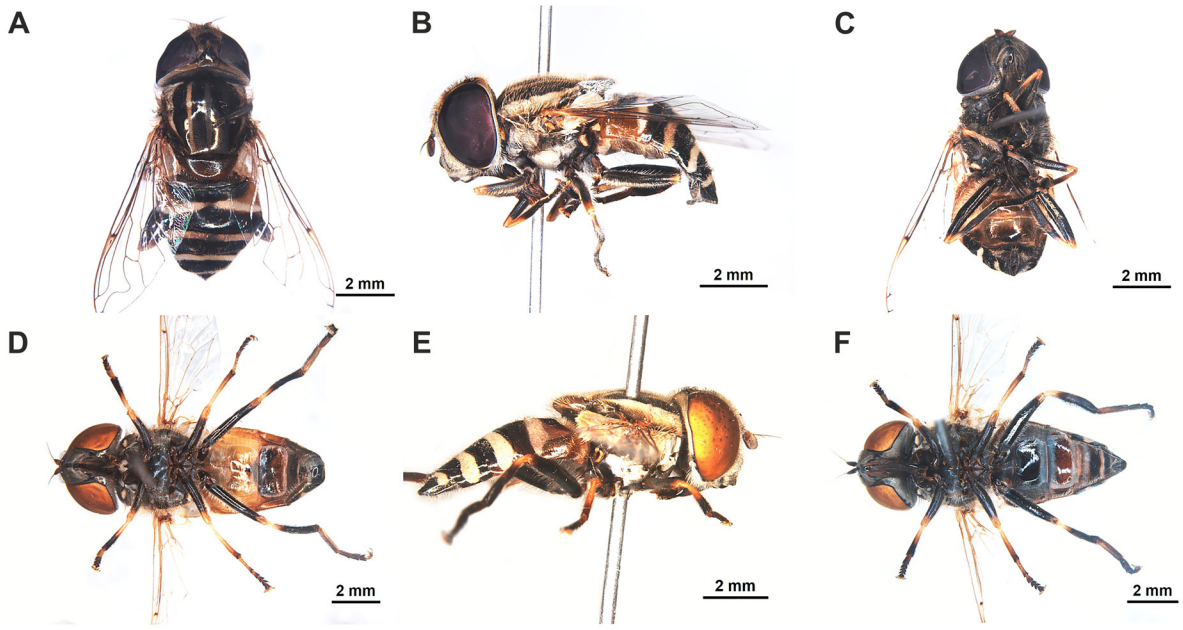

Fig. 18. A–D. *Eristalinus megacephalus* (Rossi, 1794) (NZSI). **A–C**. Female habitus. **A**. Dorsal view. **B**. Lateral view. **C**. Ventral view. **D**. Male habitus, ventral view. **E–F**. *E. tabanoides* (Jaennicke, 1867), ♀ (NZSI). **E**. Lateral habitus. **F**. Ventral habitus.

11. Scutum with longitudinal, strongly contrasting and continuous four shining black and five light yellow pruinose vittae (Fig. 14B–C) 12
– Scutum tawny with dull black vittae distinctly interrupted behind the transverse sulcus (Mutin 2020: fig. 1) ..... ***Eristalinus arulans*** (Wiedemann, 1824)

12. Femora mainly yellowish brown or orange (Fig. 16A–B) ... ***Eristalinus arvorum*** (Fabricius, 1787)
– Femora all black except at the extreme apex (Fig. 16C–D) 13

13. Abdomen short, ovate-conical (Fig. 17A–B); tarsi predominantly pale yellow, with apical 4–5 tarsomeres black (Fig. 16C–D) ..... ***Eristalinus quinquestriatus*** (Fabricius, 1794)
– Abdomen long, elongate-conical (Figs 14C, 17C); tarsi predominantly black, with only basitarsomere pale yellow on basal ¼–½ (Fig. 18C–D, F) 14

14. Males: tergum II with arcuate creamy white fascia (Smit *et al*. 2017: pls 10, 12). Females: fascia on tergum II not tapering laterally, attaining its maximum width sublaterally and reaching the lateral margins (Figs 14C, 18E) ..... ***Eristalinus tabanoides*** (Jaennicke, 1867)
– Males: tergum II without arcuate creamy white fascia (Fig. 17C). Females: fascia on tergum II tapering laterally, attaining its maximum width at middle, and not reaching the lateral margins (Fig. 18A–D) ..... ***Eristalinus megacephalus*** (Rossi, 1794)

DNA barcoding and phylogenetic analyses

The MEGAX program utilized the Kimura-2-Parameter (K2P) method to assess genetic divergences between and within species. A DNA barcode analysis technique for species differentiation has been developed to compare intraspecific and interspecific genetic divergence (bar-coding gap) (Herbert *et al*. 2003). To ensure that the COI-5′ gene is reliable for identification, intraspecific divergences should be <2% and interspecific divergences should be >2%. Intraspecific divergences ranged from 0% to 2%, and interspecific divergences ranged from 0.12% to 13.32% in the present study. Both new species of *Eristalinus* exhibited 0% intraspecific divergence and >6% interspecific divergence with other species of *Eristalinus* (Supp. file 1, Supp. file 2). These findings align with the patterns observed in DNA barcoding studies and support the phylogenetic separation identified in the tree-based analyses.

All three phylogenetic trees, including the Neighbor-Joining (NJ), Bayesian Analysis (BA) and Maximum Likelihood (ML) trees, showed congruence with each other, confirming reciprocal monophyly. The NJ tree with monophyletic separation showed that the *Eristalinus* species were accurately differentiated, proving they were correctly identified (Fig. 19). The high bootstrap values of 99–100% at the species level showed support for the unique molecular identification of the species under study. In the phylogenetic tree, *E. sapphirinus* sp. nov. showed a bootstrap support of 100%, indicating that both sexes are correctly associated. *Eristalinus brunettii* sp. nov. and *E. polychromata* also separated into two distinct clades, with strong bootstrap support of 100%. In the BA tree (Fig. 20) and ML tree (Fig. 21), the same pattern was observed. *Eristalinus brunettii* and *E. polychromata* separated out distinctly with strong bootstrap support of 100% and posterior probability values of 1.

The four delimitation methods, ABGD, ASAP, PTP and GMYC, were used for species identification, produced similar results. MOTUs without a match were not found. Out of the 10 ‘best’ partitions determined by the ASAP analysis, the sixth partition, ranked first, was selected with an ASAP score of 3.0 and a threshold distance of 0.002059. ASAP analysis formed 14 MOTUs (excluding the out-group), which was similar to the PTP analysis, which also produced 14 MOTUs (excluding the out-group). ABGD analysis yielded 17 MOTUs, which were comparable to those obtained by GMYC analysis, which also identified a similar number of MOTUs. In all the species delimitation analyses, *E. sapphirinus* sp. nov. was properly separated and showed clear delimitation from others. It formed a separate species group.

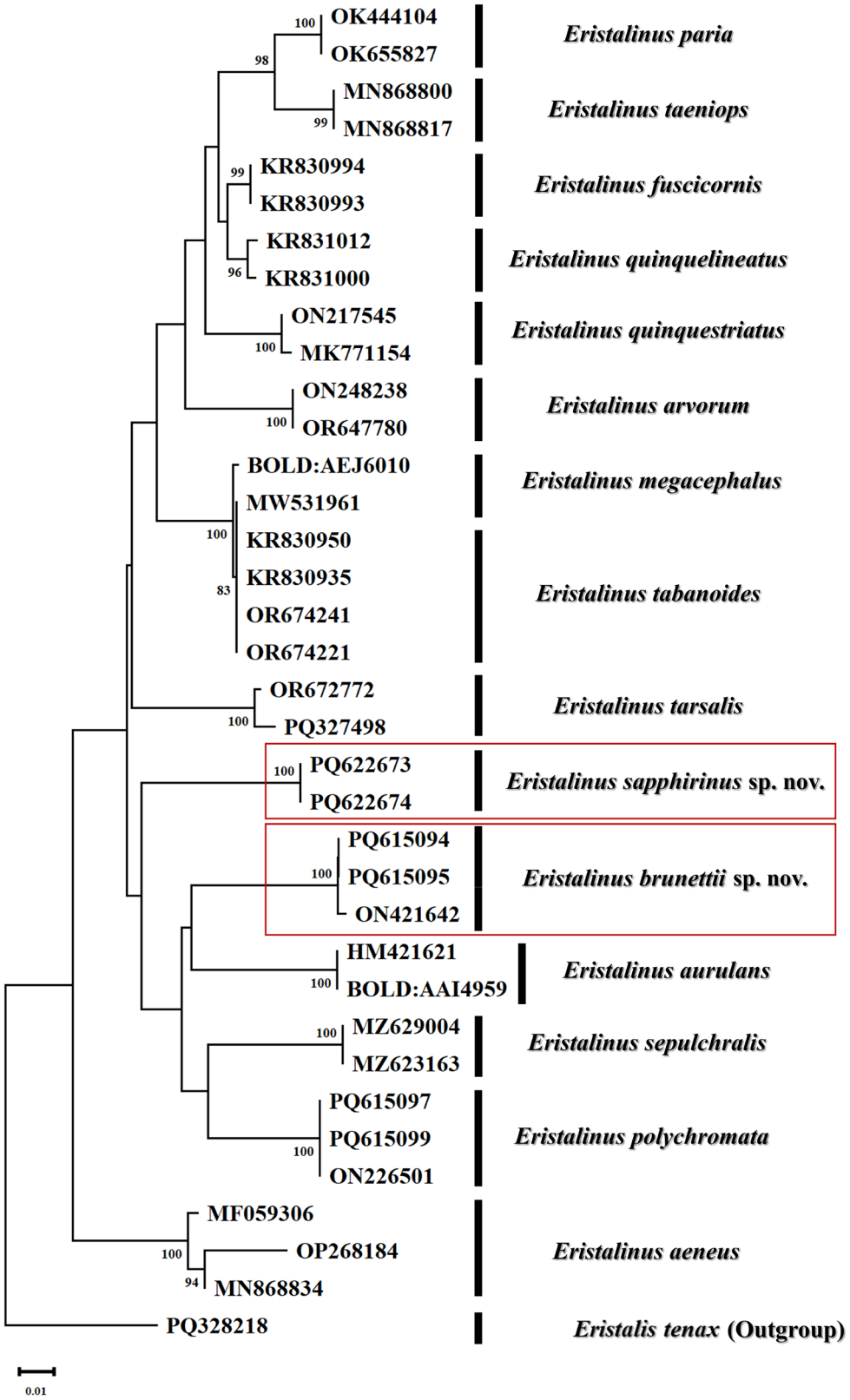

Fig. 19. Neighbour-Joining tree of the species of *Eristalinus* Rondani, 1845. The numbers indicate bootstrap values from the NJ analysis and bootstrap values of > 70.

Eristalinus brunettii sp. nov. and *E. polychromata* also differentiated into two separate species groups (Fig. 21).

Discussion

The discovery of *Eristalinus sapphirinus* sp. nov. and *Eristalinus brunettii* sp. nov. highlights the continuing underestimation of the species diversity within Indian Eristalinae. Both newly described species come from the Gangetic Plains, a region characterized by a high human population density, organic enrichment and anthropogenic disturbance. Although such environments are not generally considered centres of syrphid diversity, they are known to support a subset of scavenger eristaline taxa, whose larvae develop in organic-rich, semi-aquatic or polluted substrates (Pérez-Bañón *et al*. 2003, 2020; Campoy *et al*. 2017). Biological observations indicate differences in the vertical activity and habitat use among the species of *Eristalinus*. *Eristalinus brunettii* was predominantly observed engaging in higher flight activity and frequently occurring in the canopies of woody trees, whereas *E. polychromata* was consistently associated with low vegetation and crop fields. *Eristalinus sapphirinus* was recorded feeding near drainage channels and adjacent agricultural habitats, with females showing slow hovering behaviour. Occasional records of more than one species of *Eristalinus* from the same localities suggest overlapping habitat use at broader spatial scales; however, differences in flight height and vegetation strata may reflect microhabitat differentiation rather than direct ecological overlap. The repeated occurrence of multiple species of *Eristalinus* in close association with drainage systems, crop fields and synanthropic vegeta-

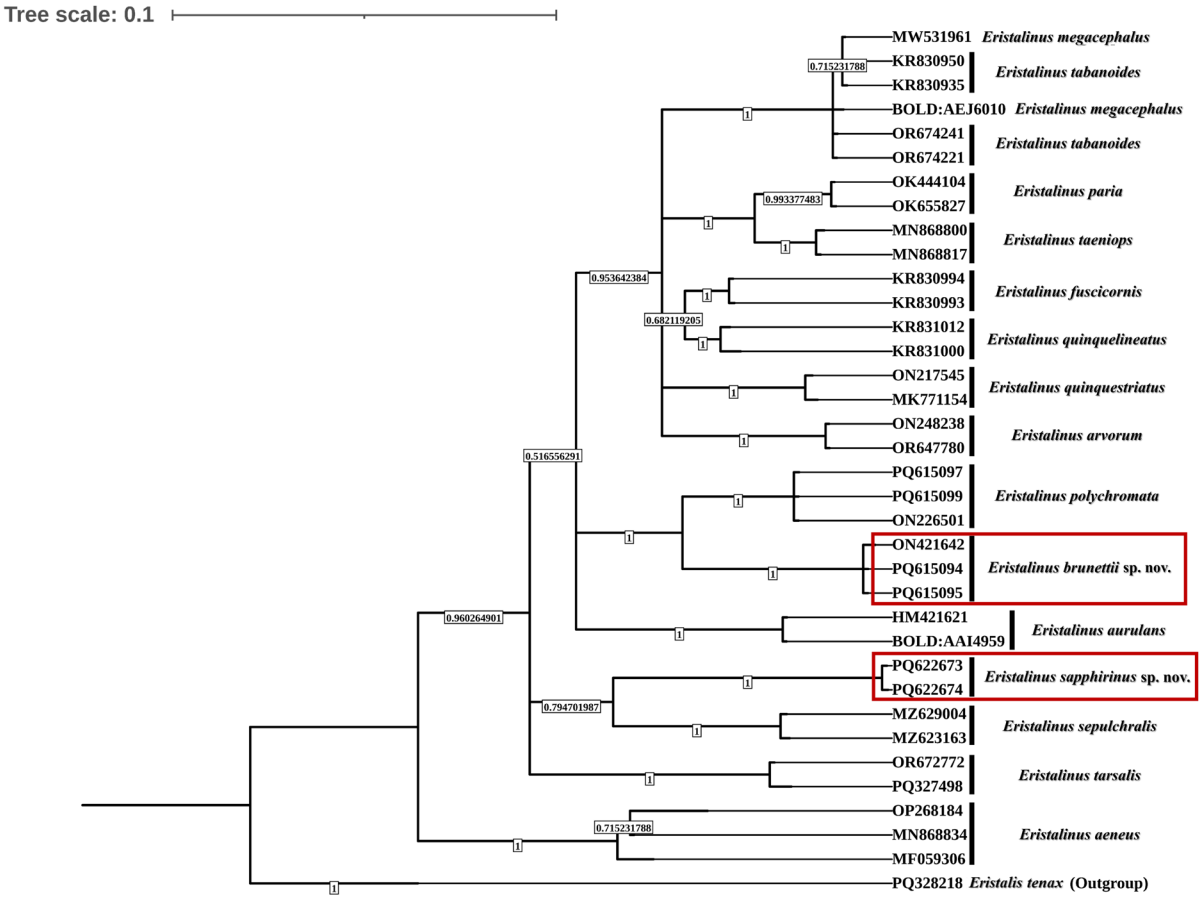

Fig. 20. Bayesian tree (BA) of the species of *Eristalinus* Rondani, 1845. The numbers indicate posterior probability values from Bayesian analysis.

tion in the present study also suggests that these modified habitats remain insufficiently surveyed for scavenger syrphids in India.

The current morphological assessment reveals that *E. brunettii* sp. nov. is closely allied to *E. polychromata*, sharing similarities in body size, habitus and abdominal colouration. However, *E. brunettii* differs consistently across several stable characters, including the width of facial vitta, colour and density of body pilosity, mesonotal colouration, and wing infuscation, supporting its recognition as a distinct taxon (Table 2). The second new taxon, *E. sapphirinus* sp. nov., shows marked association with metallic or aeneous coloured species and congeners possessing a unicoloured scutellum, in the presence of metallic sheen in mesonotum and abdomen. Although comparable to several Indian *Ersitalinus* (e.g., *E. aeneus*, *E. sepulchralis*, *E. tarsalis*, etc.), *E. sapphirinus* is uniquely characterized by a brilliant blueish black body, restricted coloured maculae on tergum II, and possession of an appendix on the vein R_{4+5}.

Male genitalia provide robust evidence for species delimitation within *Eristalinus*. The genitalia of both new species conform to the ground plan of the genus, characterized by an arched hypandrium and an elongate postgonite often bearing ventral projections (Pérez-Bañón *et al*. 2003), yet exhibit stable, species-specific modifications. In *E. brunettii* sp. nov., the surstylus displays a distinctly sinuous ventral margin medially, in contrast to the nearly straight margin in *E. polychromata* and the outwardly curved margin in *E. sapphirinus* sp. nov. (Fig. 7). Additional differences are evident in hypandrial curvature and the configuration of the postgonite projections. These characters are consistent across examined specimens and represent stable diagnostic features. More notably, the epandrium, surstylus, hypandrial curvature, and postgonite structure of the two new species and *E. polychromata* show closer resemblance

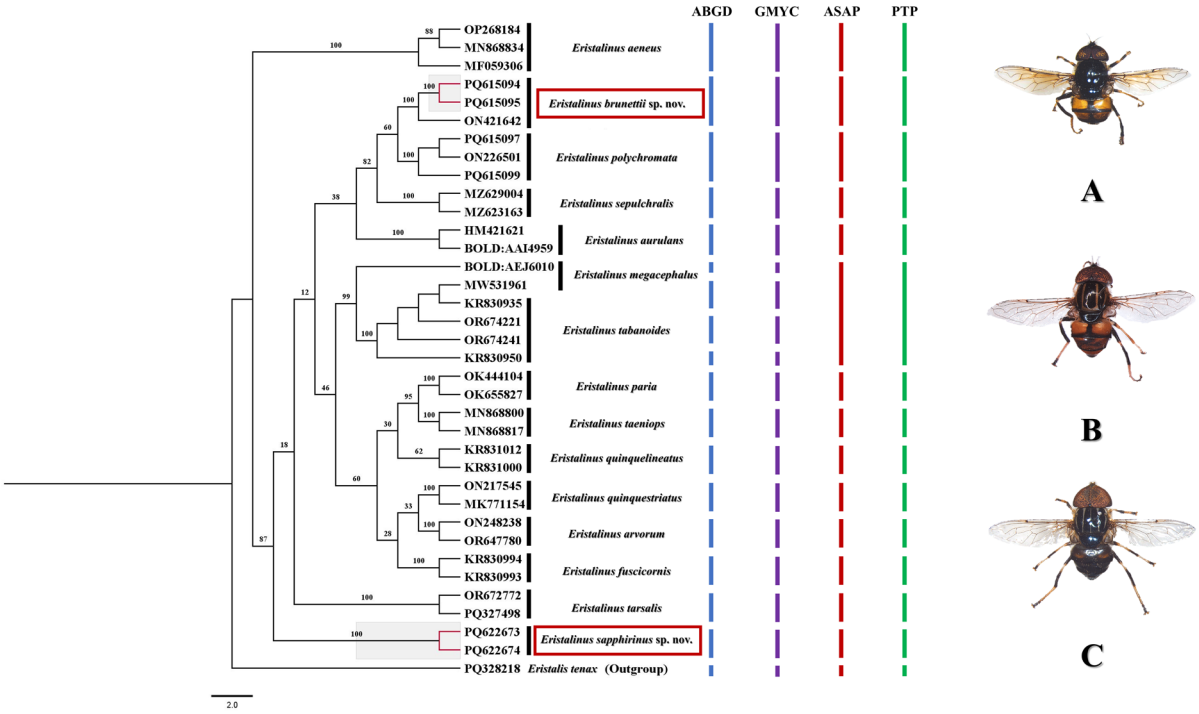

Fig. 21. Maximum Likelihood (ML) tree of 15 species of *Eristalinus* Rondani, 1845 (including 2 new species) with comparison of different species delimitation methods: Poisson Tree Processes (PTP), Generalized Mixed Yule Coalescent (GMYC), and Automatic Barcode Gap Discovery (ABGD). Images: **A**. *Eristalinus brunettii* Roy, Naskar & Banerjee sp. nov. **B**. *E. polychromata* Brunetti, 1923. **C**. *E. sapphirinus* Roy, Naskar & Banerjee sp. nov.

to *E. megacephalus* (with a partly yellow scutellum) and *E. taeniops* (subgenus *Eristalodes*) than to the aeneous-bodied species *E. aeneus* and *E. sepulchralis* (Pérez-Bañón *et al*. 2003). Interestingly, the three species bearing a shining black scutellum—*E. brunettii*, *E. polychromata* and *E. sapphirinus*—exhibit notable congruence in the overall genitalic architecture. This correspondence may suggest a closer morphological affinity among these taxa; however, evaluation of this potential grouping remains incomplete, as the male genitalia of *E. tarsalis*, another species with a black scutellum, are currently unknown. Accordingly, while the scutellar colouration appears to coincide with the genitalic similarity in part of this assemblage, its broader systematic significance within the genus requires further investigation.

Phylogenetic analyses based on mitochondrial COI sequences consistently recovered well-resolved species-level lineages within *Eristalinus*, and the overall topologies obtained from the NJ (Fig. 19), BA (Fig. 20) and ML (Fig. 21) frameworks were largely congruent. In all three analytical frameworks, most recognized species formed distinct monophyletic clusters with strong support values, indicating that mitochondrial COI provides a reliable signal for species-level identification in the genus. In particular, *E. brunettii* sp. nov. and *E. sapphirinus* sp. nov. recovered as independent lineages across all analytical approaches, and multiple species-delimitation methods (ABGD, GMYC, ASAP and PTP) consistently recognized them as separate MOTUs. The absence of detectable intraspecific divergence within each new species, with their comparatively high interspecific distances from their nearest neighbours, corroborates their evolutionary independence and supports integrative evidence for species delimitation.

Although the species-level resolution is robust, subgeneric relationships within *Eristalinus* remain comparatively weakly resolved. Previous phylogenomic studies showed that although *Eristalinus* appears to be monophyletic as a genus, its internal subgeneric divisions are not consistently supported (Sonet *et al*. 2019; Mullens *et al*. 2022; Kar *et al*. 2024). In particular, *Eristalodes* and *Merodonoides* were recovered as monophyletic in some analyses, whereas the nominal subgenus *Eristalinus* appeared paraphyletic (Mullens *et al*. 2022). In our study, *Eristalodes* has been recovered as monophyletic in the NJ (Fig. 19) and BA (Fig. 20) trees but appeared paraphyletic in the ML analysis (Fig. 21), where *E. fuscicornis* clustered within the clade of the subgenus *Eristalinus*. Species-delimitation analyses also supported the distinctness of most taxa, with each species forming a separate MOTU. However, *E. tabanoides* and *E. megacephalus* clustered together in the ASAP and PTP analyses in the ML tree (Fig. 21), a similar pattern also reported by Sonet *et al*. (2019).

Notably, the results of the molecular analyses correspond with certain morphological observations derived from the male genitalia. The genital structure of the two new species and *E. polychromata* shows similarity to that of *E. taeniops*, a representative of the subgenus *Eristalodes*. Such similarity between taxa currently assigned to different subgenera supports earlier suggestions that characters traditionally used to delimit subgenera, particularly eye patterning (maculate eyes for subgenus *Eristalinus* and fasciate eyes for subgenus *Eristalodes*), may not accurately reflect evolutionary relationships within genus *Eristalinus* (Pérez-Bañón *et al*. 2003). These genital resemblances support the molecular results and suggest that subgeneric boundaries within *Eristalinus* may be less clearly defined. Nevertheless, resolving these higher systematic relationships will require broader taxon sampling and multilocus or genome-scale datasets, as emphasized in previous studies (Sonet *et al*. 2019; Mullens *et al*. 2022). Despite these limitations, the present integrative analysis provides robust support for the recognition of the newly described taxa and contributes additional molecular and morphological data toward clarifying species boundaries within the genus.

With the description of *E. brunettii* sp. nov. and *E. sapphirinus* sp. nov., the number of species of *Eristalinus* recorded from India increases to 16. These findings highlight the importance of continued field surveys in human-modified landscapes of the Gangetic Plains, which may reveal previously undocumented taxa even in relatively well-studied groups of hoverflies. Further exploration of such

habitats may uncover additional cryptic diversity and improve our understanding of the evolution and ecology of the Indian syrphid fauna.

Acknowledgments

The authors would like to thank the Director, Zoological Survey of India, Kolkata, Ministry of Environment, Forest, and Climate Change (MOEFCC), for providing us with the necessary facilities to carry out the present work. The authors are also grateful to Dr Guru Pada Mandal, Scientist-E and Divisional-in-Charge, Entomology-B division, for his continuous support and guidance. The first author gratefully acknowledges the financial assistance under the Senior Research Fellowship (ID-201610101398) provided by the University Grants Commission (UGC), Government of India, New Delhi. We further extend our gratitude to Dr Bindarika Mukherjee for her assistance with the drawing of male genitalia and Mrs Kalpona Roy for her assistance in the sample collection.

References

Banerjee D., Kumar V., Maity A., Ghosh B., Tyagi K., Singha D., Kundu S., Laskar B., Naskar A. & Rath S. 2015. Identification through DNA barcoding of Tabanidae (Diptera) vectors of surra disease in India. *Acta Tropica* 150: 52–58. https://doi.org/10.1016/j.actatropica.2015.06.023

Becker T. 1922. Wissenschaftliche Ergebnisse der mit Unterstützung der Akademie der Wissenschaften in Wien aus der Erbschaft Treitl von F. Werner unternommenen zoologischen Expedition nach dem anglo-ägyptischen Sudan (Kordofan) 1914. VI. Diptera. Mit Beiträge von O. Duda (Habelschwerdt), P. Stein (Treptow), J. Villeneuve (Rambouillet), and H. Zerny (Wien). *Denkschriften der Kaiserlichen Akademie der Wissenschaften, Mathematisch-Naturwissenschaftliche Classe* 98 [1923]: 57–82. [publication date 27 Apr. 1922]. Available from https://www.biodiversitylibrary.org/page/35811330 [accessed 10 Apr. 2026].

Bigot J.M.F. 1880. Diptères nouveaux ou peu connus. 14^{e} partie. XXI. Syrphidi (mihi). — Genre *Eristalis* (Fabr.). *Annales de la Société entomologique de France*, *Series 5* 10: 213–230.
Available from https://www.biodiversitylibrary.org/page/8232061 [accessed 10 Apr. 2026].

Brunetti E. 1923. Family Syrphidae. *In*: Shipley A.E. & Scott H. (eds) *The Fauna of British India Including Ceylon and Burmam Diptera Vol. III. Pipunculidae, Syrphidae, Conopidae, Oestridae*: 23–340. Taylor & Francis, London. Available from https://www.biodiversitylibrary.org/page/9472589 [accessed 10 Apr. 2026].

Campoy A., Pérez-Bañón C., Nielsen T.R. & Rojo S. 2017. Micromorphology of egg and larva of *Eristalis fratercula*, with an updated key of *Eristalis* species with known third instar larvae (Diptera: Syrphidae). *Acta Entomologica Musei Nationalis Pragae* 57 (1): 215–227. https://doi.org/10.1515/aemnp-2017-0070

Choi D.S. & Han H.Y. 2004. Redescription of *Graptomyza ihai* Shiraki (Diptera, Syrphidae), first recorded genus and species in Korea. *Entomological Research* 34 (1): 1–5.

Curran C.H. 1931. Records and descriptions of Syrphidae from North Borneo including Mt. Kinabalu. *Journal of the Federate Malay States Museum* 16: 333–376.

Darriba D., Taboada G.L., Doallo R. & Posada D. 2012. jModelTest 2: more models, new heuristics and parallel computing. *Nature Methods* 9 (8): 772–772. https://doi.org/10.1038/nmeth.2109

Dunn L., Lequerica M., Reid C.R. & Latty T. 2020. Dual ecosystem services of syrphid flies (Diptera: Syrphidae): pollinators and biological control agents. *Pest Management Science* 76 (6): 1973–1979. https://doi.org/10.1002/ps.5807

Dutta M. & Chakraborti M. 1986. On collections of flower flies (Diptera: Syrphidae) from South India. *Records of the Zoological Survey of India* 83 (1&2): 53–67.

Fabricius J.C. 1781. *Species insectorum exhibentes eorum differentias specificas, synonyma auctorum, loca natalia, metamorphosin adjectis observationibus, descriptionibus. Tomus II*. C.E. Bohnii, Hamburg & Kiel [Hamburgi et Kilonii]. https://doi.org/10.5962/bhl.title.36509

Fabricius J.C. 1787. *Mantissa insectorum sistens species nuper detectas. Vol. 2*. C.G. Proft, Copenhagen [Hafniae]. https://doi.org/10.5962/bhl.title.36471

Fabricius J.C. 1794. *Entomologia systematica emendata et aucta. Secundum classes, ordines, genera, species adjectis synonimis, locis, observationibus, descriptionibus. Tom. IV.* C.G. Proft, Fil. et Soc., Copenhagen [Hafniae]. https://doi.org/10.5962/bhl.title.125869

Folmer O., Black M., Hoeh W., Lutz R. & Vrijenhoek R. 1994. DNA primers for amplification of mitochondrial cytochrome c oxidase subunit I from diverse metazoan invertebrates. *Molecular Marine Biology and Biotechnology* 3 (5): 294–299.

Ghosh D., Kar O., Pramanik D., Mukherjee A., Sarkar S., Mukherjee K., Naskar A. & Banerjee D. 2022. Molecular identification and characterization of muscid flies (Diptera: Muscidae) of medico-veterinary importance from the Gangetic plains of Eastern India. *International Journal of Tropical Insect Science* 42 (6): 3759–3769. https://doi.org/10.1007/s42690-022-00900-9

Heo C.C., Rahimi R., Mengual X., M. Isa M.S., Zainal S., Khofar P.N. & Nazni W.A. 2020. *Eristalinus arvorum* (Fabricius, 1787) (Diptera: Syrphidae) in human skull: a new fly species of forensic importance. *Journal of Forensic Sciences* 65 (1): 276–282. https://doi.org/10.1111/1556-4029.14128

Hebert P.D.N., Cywinska A., Ball S.L. & DeWaard J.R. 2003. Biological identifications through DNA barcodes. *Proceedings of the Royal Society B: Biological Sciences* 270 (1512): 313–321. https://doi.org/10.1098/rspb.2002.2218

Jaennicke F. 1867. Neue exotische Dipteren. *Abhandlungen, herausgegeben von der Senckenbergischen Naturforschenden Gesellschaft* 6: 311–407.
Available from https://www.biodiversitylibrary.org/page/26186732 [accessed 10 Apr. 2026].

Johnson M., Zaretskaya I., Raytselis Y., Merezhuk Y., McGinnis S. & Madden T.L. 2008. NCBI BLAST: A better web interface. *Nucleic Acids Research 36* (suppl_2): W5–W9. https://doi.org/10.1093/nar/gkn201

Kahanpää J. 2021. A new character for identification of females of *Eristalinus aeneus* (Scopoli, 1763) and *E. sepulchralis* (Linnaeus, 1758) (Diptera: Syrphidae). *Luomus Sahlbergia* 27 (2): 11–13.

Ka-Lun K.W. 2022. The hoverfly genus *Eristalinus* Rondani, 1845 (Diptera: Syrphidae) in Hong Kong (Part 1). *Hong Kong Entomological Society* 14 (2): 15–21.

Kar O., Ghosh D., Mukherjee A., Mukherjee K., Pramanik D., Sarkar S., Sengupta J., Naskar A. & Banerjee D. 2024. Molecular identification of ecologically relevant hoverflies (Diptera, Syrphidae) from eastern India. *Entomon* 49 (3): 295–308. https://doi.org/10.33307/entomon.v49i3.1250

Karsch F.A. 1887. Dipteren von Pungo-Andongo, gesammelt von Herrn Major Alexander von Homeyer [concl.]. *Entomologische Nachrichten* 13: 97–105.
Available from https://www.biodiversitylibrary.org/page/32444246 [accessed 10 Apr. 2026].

Kondo T., Rosero R. & Gaviria J. 2024. *Eristalinus taeniops* (Wiedemann, 1818) (Diptera: Syrphidae), an exotic flower fly rapidly spreading in South America: A review. *Revista Chilena de Entomología* 50 (3): 589–599. https://doi.org/10.35249/rche.50.3.24.17

Kumar S., Stecher G., Li M., Knyaz C. & Tamura K. 2018. MEGA X: Molecular Evolutionary Genetics Analysis across computing platforms. *Molecular Biology and Evolution* 35 (6): 1547–1549. https://doi.org/10.1093/molbev/msy096

Kundu S., Chandra K., Tyagi K., Pakrashi A. & Kumar V. 2019. DNA barcoding of freshwater fishes from Brahmaputra River in Eastern Himalaya biodiversity hotspot. *Mitochondrial DNA B* 4 (2): 2411–2419. https://doi.org/10.1080/23802359.2019.1637290

Letunic I. & Bork P. 2021. Interactive Tree of Life (iTOL) v5: An online tool for phylogenetic tree display and annotation. *Nucleic Acids Research* 49 (1): 293–296. https://doi.org/10.1093/nar/gkab301

Linnaeus C. 1758. *Systema Naturae per regna tria naturae, secundum classes, ordines, genera, species, cum characteribus, differentiis, synonymis, locis. Editio decima, reformata. Tomus I.* Laurentii Salvii, Stockholm [Holmiae]. https://doi.org/10.5962/bhl.title.542

Macquart P.J.M. 1834. *Histoire naturelle des insectes. Diptères*. *Tome premiere*. Roret, Paris. https://doi.org/10.5962/bhl.title.14274

Macquart P.J.M. 1855 [1854]. Diptères exotiques nouveaux ou peu connus. 5.e supplément. *Mémoires de la Société royale des Sciences, Agriculture et des Arts, de Lille, Series 2* 1: 25–156. https://www.biodiversitylibrary.org/item/23242#page/37

Mik J. 1897. Einige Bemerkungen zur Dipteren-Familie der Syrphiden [concl.]. *Wiener Entomologische Zeitung* 16: 113–119.
Available from https://www.biodiversitylibrary.org/page/12065766 [accessed 10 Apr. 2026].

Miller M.A., Pfeiffer W. & Schwartz T. 2010. Creating the CIPRES Science Gateway for inference of large phylogenetic trees. *2010 Gateway Computing Environments Workshop (GCE), New Orleans, LA, USA*: 1–8. https://doi.org/10.1109/GCE.2010.5676129

Miller M.A., Pfeiffer W. & Schwartz T. 2012. The CIPRES science gateway: enabling high-impact science for phylogenetics researchers with limited resources. *Proceedings of the 1st Conference of the Extreme Science and Engineering Discovery Environment: Bridging from the extreme to the campus and beyond*: 1–8. Association for Computing Machinery, Chicago. https://doi.org/10.1145/2335755.2335836

Minh B.Q., Schmidt H.A., Chernomor O., Schrempf D., Woodhams M.D., von Haeseler A. & Lanfear R. 2020. IQ-TREE 2: New models and efficient methods for phylogenetic inference in the genomic era. *Molecular Biology and Evolution* 37 (5): 1530–1534. https://doi.org/10.1093/molbev/msaa015

Mitra B., Mukherjee M. & Banerjee D. 2008. A check-list of hoverflies (Diptera: Syrphidae) of Eastern Himalayas. *Records of the Zoological Survey of India* Occasional Paper No. 284: 1–47.

Mitra B., Roy S., Imam I. & Ghosh M. 2015. A review of the hover flies (Syrphidae: Diptera) from India. *International Journal of Fauna and Biological Studies* 2: 61–73.

Mullens N., Sonet G., Virgilio M., Goergen G., Janssens S.B., De Meyer M. & Jordaens K. 2022. Systematics of Afrotropical Eristalinae (Diptera: Syrphidae) using mitochondrial phylogenomics. *Systematic Entomology* 47 (2): 315–328. https://doi.org/10.1111/syen.12532

Mutin V. A. 2020. New data on hoverflies (Diptera: Syrphidae) from Russian Far East. *Far East Entomologist* 403: 20–24.

Pérez-Bañón C., Rojo S., Ståhls G. & Marcos-García M. 2003. Taxonomy of European *Eristalinus* (Diptera: Syrphidae) based on larval morphology and molecular data. *European Journal of Entomology* 100: 417–428. https://doi.org/10.14411/eje.2003.064

Pérez-Bañón C., Rojas C., Vargas M., Mengual X. & Rojo S. 2020. A world review of reported myiases caused by flower flies (Diptera: Syrphidae), including the first case of human myiasis from *Palpada scutellaris* (Fabricius, 1805). *Parasitology Research* 119 (6): 815–840.
https://doi.org/10.1007/s00436-020-06616-4

Pons J., Barraclough T.G., Gomez-Zurita J., Cardoso A., Duran D.P., Hazell S., Kamoun S., Sumlin W.D. & Vogler A.P. 2006. Sequence-based species delimitation for the DNA taxonomy of undescribed insects. *Systematic Biology* 55 (4): 595–609. https://doi.org/10.1080/10635150600852011

Puillandre N., Lambert A., Brouillet S. & Achaz G. 2012. ABGD, Automatic Barcode Gap Discovery for primary species delimitation. *Molecular Ecology* 21 (8): 1864–1877. https://doi.org/10.1111/j.1365-294X.2011.05239.x

Puillandre N., Brouillet S. & Achaz G. 2021. ASAP: assemble species by automatic partitioning. *Molecular Ecology Resources* 21 (2): 609–620. https://doi.org/10.1111/1755-0998

Ricarte A., Nedeljković Z., Rotheray G.E., Lyszkowski R., Hancock E., Watt K., Hewitt S., Horsfield D. & Wilkinson G. 2012. Syrphidae (Diptera) from the Greek island of Lesvos, with description of two new species. *Zootaxa* 3175: 1–23. https://doi.org/10.11646/zootaxa.3175.1.1

Rondani C. 1845. Ordinamento sistematico dei generi italiani degli insetti ditteri. *Nuovi Annali delle Scienze Naturali e Rendiconto delle Sessioni della Società Agraria e dell'Accademia delle Scienze dell'Istituto di Bologna*, Serie 2 2: 443–459.
Available from https://www.biodiversitylibrary.org/page/9295449 [accessed 10 Apr. 2026].

Ronquist F., Teslenko M., van der Mark P., Ayres D.L., Darling A., Höhna S., Larget B., Liu L., Suchard M.A. & Huelsenbeck J.P. 2012. MrBayes 3.2: efficient Bayesian phylogenetic inference and model choice across a large model space. *Systematic Biology* 61 (3): 539–542. https://doi.org/10.1093/sysbio/sys029

Rossi P. 1794. *Mantissa insectorum, exhibens species nuper in Etruria collectas, adjectis faunae etruscae illustrationibus ac emendationibus. Tomus secundus*. Polloni, Pisa. https://doi.org/10.5962/bhl.title.49449

Rotondi B.A.R., Videla M., Beccacece H.M. & Fenoglio M.S. 2020. New records of the exotic band-eyed drone fly, *Eristalinus taeniops* (Wiedemann, 1818) (Diptera, Syrphidae), in Argentina. *Check List* 16 (6): 1523–1529. https://doi.org/10.15560/16.6.1523

Scopoli J.A. 1763. *Entomologia carniolica exhibens insecta carnioliae indigena et distribute in ordines, genera, species, varietates. Methodo Linnaeana*. Trattner, Vienna [Vindobonae]. https://doi.org/10.5962/bhl.title.119976

Séguy E. 1951. Trois nouveaux syrphides de Madagascar (Dipt.). *Revue française d'Entomologie* 18: 14–18.

Sengupta J., Roy B., Naskar A. & Banerjee D. 2024. A catalogue of Indian hoverflies (Insecta: Diptera: Syrphidae). *Records of the Zoological Survey of India*, *Occasional Paper* 420: 1–198.

Smit J.T., van Harten A. & Ketelaar R. 2017. Order Diptera, family Syrphidae. The hoverflies of the Arabian Peninsula. *In*: van Harten A. (ed.) *Arthropod Fauna of the UAE, Volume 6*: 572–612. Department of The President's Affairs, Abu Dhabi.

Sonet G., De Smet Y., Tang M., Virgilio M., Young A.D., Skevington J.H., Mengual X., Backeljau T., Liu S., Zhou X. & De Meyer M. 2019. First mitochondrial genomes of five hoverfly species of the genus *Eristalinus* (Diptera: Syrphidae). *Genome* 62 (10): 677–687. https://doi.org/10.1139/GEN-2019-0009

Ssymank A., Jordaens K., Meyer M.D., Reemer M. & Rotheray G.E. 2021. 60. Syrphidae (flower flies or hoverflies). *In*: Kirk-Spriggs A.H. & Sinclair B.J. (eds) *Manual of Afrotropical Diptera. Volume 3. Brachycera–Cyclorrhapha, excluding Calyptratae. Suricata 8*: 1439–1492. South African National Biodiversity Institute, Pretoria. Available from https://www.biodiversitylibrary.org/page/64825900 [accessed 10 Apr. 2026].

van Steenis J., Miranda G.F.G., Tot T., Mengual X. & Skevington J.H. 2023. Glossary of morphological terminology of adult Syrphidae (Diptera): an update and extension. *Journaal van Syrphidae* 2 (4): 1–99. https://doi.org/10.55710/1.AIMS1978

Thompson F.C. & Rotheray G.E. 1998. Family Syrphidae. *In*: Papp L. & Darvas B. (eds) *Manual of Palaearctic Diptera, Volume 3*: 81–139. Science Herald, Budapest.

Wiedemann C.R.W. 1818. Neue Insecten vom Vorgebirge der guten Hoffnung. *Zoologisches Magazin* 1 (2): 40–48. Available from https://www.biodiversitylibrary.org/page/14282426 [accessed 10 Apr. 2026].

Wiedemann C.R.W. 1824. *Munus rectoris in Academia Christiana Albertina aditurus analecta entomologica ex Museo Regio Havniensi maximw congesta profert iconibusque illustrat*. Eregio typoguapheo scholarum, Kiel [Kiliae]. https://doi.org/10.5962/bhl.title.77322

Zhang J., Kapli P., Pavlidis P. & Stamatakis A. 2013. A general species delimitation method with applications to phylogenetic placements. *Bioinformatics* 29 (22): 2869–2876. https://doi.org/10.1093/bioinformatics/btt499

Printed versions of all papers are deposited in the libraries of two of the institutes that are members of the *EJT* consortium: Muséum national d'Histoire naturelle, Paris, France and Royal Museum for Central Africa, Tervuren, Belgium. The other members of the consortium are: Royal Belgian Institute of Natural Sciences, Brussels, Belgium; Meise Botanic Garden, Meise, Belgium; Natural History Museum of Denmark, Copenhagen, Denmark; Naturalis Biodiversity Center, Leiden, the Netherlands; Museo Nacional de Ciencias Naturales-CSIC, Madrid, Spain; Leibniz Institute for the Analysis of Biodiversity Change, Bonn – Hamburg, Germany; National Museum of the Czech Republic, Prague, Czech Republic; The Steinhardt Museum of Natural History, Tel Aviv, Israël.

Supplementary files

Supp. file 1. Average interspecific genetic distances (K2P model) of the COI-5′ sequences of selected species of *Eristalinus* Rondani, 1845. https://doi.org/10.5852/ejt.2026.1062.3286.14491

Supp. file 2. Average intraspecific genetic distances (K2P model) of the COI-5′ sequences of selected species of *Eristalinus* Rondani, 1845. https://doi.org/10.5852/ejt.2026.1062.3286.14492